Mechanical Properties of Bioengineered Corneal Stroma

ADVANCED HEALTHCARE MATERIALS
www.advhealthmat.de

Mechanical Properties of Bioengineered Corneal Stroma

*Nello Formisano, Cas van der Putten, Rhiannon Grant, Gozde Sahin, Roman K. Truckenmüller, Carlijn V. C. Bouten, Nicholas A. Kurniawan, and Stefan Giselbrecht**

For the majority of patients with severe corneal injury or disease, corneal transplantation is the only suitable treatment option. Unfortunately, the demand for donor corneas greatly exceeds the availability. To overcome shortage issues, a myriad of bioengineered constructs have been developed as mimetics of the corneal stroma over the last few decades. Despite the sheer number of bioengineered stromas developed , these implants fail clinical trials exhibiting poor tissue integration and adverse effects in vivo. Such shortcomings can partially be ascribed to poor biomechanical performance. In this review, existing approaches for bioengineering corneal stromal constructs and their mechanical properties are described. The information collected in this review can be used to critically analyze the biomechanical properties of future stromal constructs, which are often overlooked, but can determine the failure or success of corresponding implants.

1. Introduction

Corneal transplants from deceased human donors are the only curative form of treatment currently available for patients at risk of blindness resulting from corneal disease or injury. However, donor tissues are unavailable for over 98.5% of patients worldwide,[1] creating an urgent need for alternative solutions. Despite significant scientific progress in recent decades, successful biomimetic alternatives intended as biocompatible, functioning and structurally solid constructs, have not yet been integrated into routine clinical practice.

N. Formisano, R. Grant, G. Sahin, R. K. Truckenmüller, S. Giselbrecht
Department of Instructive Biomaterials Engineering
MERLN Institute for Technology-Inspired Regenerative Medicine
Maastricht University
Maastricht 6229 ER, The Netherlands
E-mail: s.giselbrecht@maastrichtuniversity.nl
C. van der Putten, C. V. C. Bouten, N. A. Kurniawan
Department of Biomedical Engineering
Eindhoven University of Technology
Eindhoven 5612 AP, The Netherlands

The ORCID identification number(s) for the author(s) of this article can be found under https://doi.org/10.1002/adhm.202100972

DOI: 10.1002/adhm.202100972

For patients with severe stromal injury for whom transplants are unavailable or fail, subsequent treatment options are limited. The regeneration process in vivo often results in uncontrolled production of disorganized fibrotic tissue, leading to decreased visual performance (**Figure 1**). Especially in the case of larger stromal defects or disease, a controlled regeneration process is favorable in order to restore visual performance. Pharmaceutical interventions can slow disease progression, but not restore vision.[2] In these cases, an artificial cornea—a full thickness, completely artificial "window"—can be sutured into place as a replacement. Such artificial corneas[3–10] are neither intended to provide a means to restore the damaged cornea to a structure/function existing prior the injury nor to support self-regeneration of the native tissue. They rather provide a last avenue to hopefully preserve a minimum functionality of the cornea in otherwise untreatable patients. However, artificial corneas are often accompanied by catastrophic adverse events including immune reactions and rejection, alterations in oxygen permeability, changes in the refractive index of the cornea due to alteration of its curvature and haze caused by scar tissue at the implant border that can lead to complete loss of the implant and subsequently of vision.[4,11–13]

To provide more favorable alternatives, ophthalmologists and bioengineers invest large amounts of resources in search of engineered constructs that are able to integrate more favorably into the patient's eye and perhaps trigger a self-regeneration process of the compromised tissue. To find solutions that could restore patient vision successfully, a large number of natural and synthetic materials as well as various fabrication processes are explored.

The cornea is not only responsible for converging light into the eye but, by interfacing with the external environment, it also provides protection and stability to the eye, acting as a barrier to external threats. Therefore, the biomechanics of this tissue is crucial to ensure that the cornea can fulfil its function. Transparency and biocompatibility are usually successfully addressed in the design of bioengineered stroma (in this review also referred to as "stromal constructs"). However, their mechanical properties are often overlooked, increasing the failure rate of otherwise promising strategies. Failing to provide adequate mechanical stability, in clinical trials, these implants eventually cause adverse events that can ultimately compromise the corneal integrity and eventually the patient's vision. Changes in mechanical

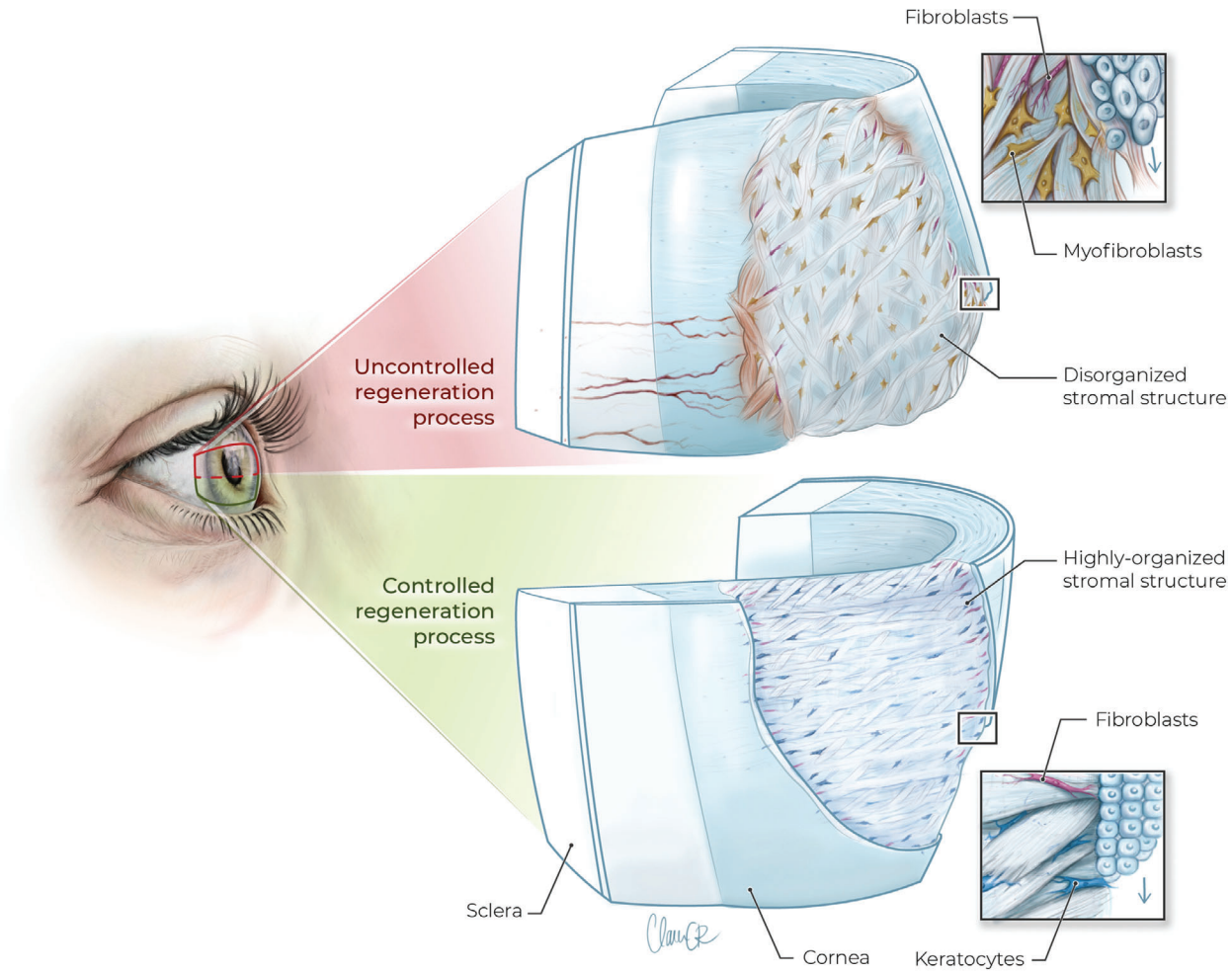

Figure 1. Schematic illustration of an injured human cornea undergoing either uncontrolled or controlled regeneration of the stroma. An uncontrolled regeneration process (top half of the illustration) can be caused, for instance, by an untreated severe injury of the stroma or following implantation of an unsuitable stromal construct, which causes an irreversible keratocyte-to-(myo)fibroblast transition as well as disorganized extracellular matrix (ECM) production. A controlled regeneration process (bottom half of the illustration) can be aided by a suitable bioengineered stromal implant that integrates well into the hosting tissue and therefore fosters native keratocyte infiltration, reversible keratocyte-to-fibroblast transition as well as a slow and organized ECM deposition and replacement.

properties of the stroma are associated with pathologies, such as ectasias, which can lead to visual loss.[14–23] In addition, surgical handling and implantation (e.g., suturing) as well as long-term integration of the stromal replacement in the human eye are strongly dependent on the mechanical characteristics of the constructs as corneal cells are known to respond to mechanical characteristics of their extracellular matrix (ECM).[24]

In this review, we address the mechanical properties of the corneal stroma and provide an overview of the existing strategies for engineering stromal constructs, focusing on the mechanical properties that they exhibit. Mechanical properties of stromal constructs are not always addressed in existing studies. Therefore, this review is not meant to provide a comprehensive overview of all the stromal constructs available but rather on those where the corresponding reports provide a quantification of their mechanical properties. In order to provide a relatively comparative set of data, we have collected studies of corneal constructs that reported two of the most commonly assessed mechanical properties, namely Young's modulus and ultimate tensile strength. Altogether, this review provides the reader with a better understanding of the efficacy and limitations of strategies for bioengineered stroma in terms of mechanical properties. Furthermore, it shall inform on the different tools available for tailoring these properties in future studies in the corneal field.

2. Characteristics of the Cornea and Corneal Stroma

2.1. Corneal Anatomy

The cornea is a homogenously stratified tissue positioned at the outermost part of the eye, covered by the tear film. The main

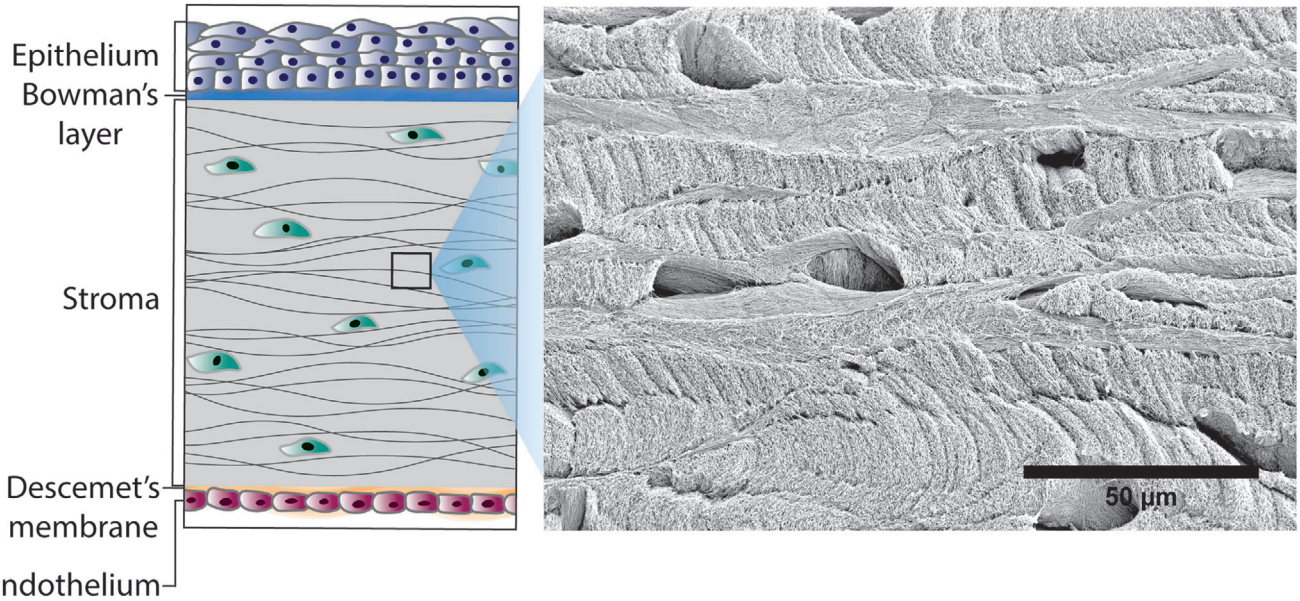

Figure 2. On the left, a schematic cross-sectional representation of the corneal anatomy illustrates the five main layers of the cornea: starting from the top: the epithelium (green), the Bowman's layer, the stroma (gray), the Descemet's membrane and the endothelium (red). On the right, a scanning electron microscopy (SEM) image of a cross section of the corneal stroma shows the organization of the collagen lamellae within the stroma (original work by the authors). Briefly, the tissue was decellularized in 10% sodium hydroxide solution (Merck) at room temperature for 6 days before it was fixed with 1% osmium tetroxide (Electron Microscopy Sciences), dehydrated in a graded series of ethanol (70%–90%–100%, Merck) and cut with a razor blade. After coating with 10 nm gold in a sputter coater (Cressington 108auto), it was transferred to a Scios DualBeam SEM (magnification 2500, 5 kV, ThermoFisher Scientific) for imaging.

function of the cornea is to protect inner parts of the eye and to refract light from the external world toward the retina, allowing vision. The cornea alone constitutes approximately two-thirds of the refractive power of the eye. It ensures maximal focus of light on the retinal surface and, at the same time, minimizes light scattering and transmission losses.[25] For this reason, a damaged or diseased cornea results in visual impairment or blindness.

In adults, the cornea extends with an oval shape measuring 11–12 mm horizontally and 10–11 mm vertically. Its thickness varies between around 500 µm in the center of the cornea and 650 µm in its periphery. The cornea consists of several layers (**Figure 2**). Externally, 6–8 epithelial cell layers form the protective corneal epithelium. Proceeding inward, an acellular 8–10 µm thin layer of collagen type I and V, called "Bowman's layer," separates the epithelium from the corneal stroma.[26] The corneal stroma is backed by the Descemet's membrane, a 10–12 µm thick basement layer of laminin, fibronectin, collagens IV and VIII upon which the corneal endothelium resides. This endothelium is a one cell thick layer of hexagonally shaped endothelial cells, which measures 4–6 µm in cross-section and allows highly controlled permeation of water, ions and metabolites to the rest of the cornea.[27]

2.2. Structure and Function of the Corneal Stroma

The corneal stroma constitutes over 90% of the thickness of the cornea and therefore it largely affects the corneal function as well as its integrity and biomechanics. In particular, the intrinsic characteristics of the stroma ultimately impact on the corneal transparency, strength, nutrient transport and curvature.

The corneal stroma is a highly organized structure containing densely packed collagen type I lamellae in a heterodimeric complex with collagens type V and VI. The stroma is also a highly hydrated tissue, containing ≈78% water. The collagen complexes are surrounded by specialized proteoglycans, such as keratocan, mimecan, lumican and decorin. The diameter of a single collagen fibril ranges between 22.5 and 35 nm with gaps between fibrils of around 41.5 nm. Approximately 200 highly organized sheets of these collagen lamellae are arranged on planes parallel to the corneal surface. The collagen fibrils within successive lamellae are oriented in an orthogonal fashion. Such precise organization and hydration confers specific mechanical strength to the cornea and is integral to its ability to refract light.[28] Additionally, this arrangement helps the cornea to withstand an intraocular pressure of 10–20 mm Hg.[29]

The collagen lamellae in the anterior of the stroma, proximal to Bowman's layer, are more densely packed, drier and stiffer in contrast to the lamellae in the posterior region of the cornea. This difference in hydration, which is due to the proximity of the anterior region to the drier external environment and of the posterior region to the aqueous humor, generates a gradient of rigidity, which eventually leads to the formation of the characteristic corneal curvature.[30] The barrier function conferred by the Bowman's layer and Descemet's membrane prevents excessive swelling of the cornea and consequent loss of transparency.[31] Although some studies show evidence that a lateral flow of fluid carrying ions and metabolites exists in the cornea,[31,32] its extent can be neglected compared to the anterior-to-posterior flow. This flow

is estimated to be about 20 μm h^{-1} of fluid from the posterior region toward the tear film, where eventually fluids leave the cornea by evaporation, and 40 μm h^{-1} in the opposite direction,[31] where fluids enter the aqueous humor, creating an overall compression force within the stroma. The consideration of this compression force and fluid flow across the stroma is crucial for the design of stromal constructs. Aberrant permeability could jeopardize a transplant due to either insufficient transport of nutrients, oxygen and ions across the implant or excess of fluid transport with opacification of the cornea as a consequence.[31]

The stroma is sparsely populated by keratocytes, which account for 5–10% of its total volume. These keratocytes produce key ECM components, such as collagen type I, proteoglycans such as keratan sulfate and dermatan sulfate, and matrix metalloproteinases.[33,34] Keratocytes are distributed with higher density in the anterior region of the stroma. They are characterized by long dendritic protrusions that allow them to sense foreign objects, injuries and other cells in the surrounding area. Corneal keratocytes continuously regenerate the collagen in the stroma and it is estimated that a complete turnover of collagen is obtained in a timeframe of several years.[35] Such a slow process is thought to underlie the successful organization of the stroma and the generation of the lamellae structures. Contrarily, a fast healing/collagen production response may be the cause of disorganized collagen deposition with consequent scar formation and loss of transparency.[36]

During trauma or infectious disease of the cornea, keratocytes undergo metabolic activation, switching to a fibroblastic phenotype that triggers cell migration, proliferation and fast/intense collagen production.[38] The process of keratocyte activation is generally reversible, however, if the injury exceeds the healing power of the cornea, keratocytes can undergo an irreversible transformation to myofibroblasts. This can lead to uncontrolled cell proliferation, migration, and collagen production, and therefore to permanent scarring and opacification (Figure 1).[37]

Such characteristics of the corneal stroma and of the cells populating it suggest that a promising bioengineered implant should possess several features: on the one hand, it has to restore a mechanically stable and functional environment, which also ensures adequate transmission of light and flow of fluids including nutrients; on the other hand, it has to allow an organized and gradual infiltration of native keratocytes into the construct and provide them with a suitable environment able to trigger self-remodeling of the damaged tissue rather than uncontrollable and irreversible response of hosting cells.

2.3. Mechanical Characteristics of the Corneal Stroma and the Impact on Corneal Keratocytes

The precise architecture and composition of the stroma, both at microscopic and macroscopic level, are responsible for its mechanical properties, such as strength, elasticity and viscosity. In particular, collagen is responsible for conferring strength and elasticity, while cellular components and proteoglycans confer viscoelastic properties to the stroma (and eventually to the whole cornea).[38] Therefore, in bioengineered corneal stroma that lack the cellular component (which represent the majority of studies in corneal stroma engineering) viscoelastic properties can be neglected, whereas strength and elasticity can be considered as more relevant. In existing studies quantifying the mechanical properties of bioengineered stroma, the assessment is mostly based on the measurements of the following two values: the Young's modulus and the ultimate tensile strength, as both mechanical characteristics are influential to the corneal strength, elasticity, cell behavior and impact suture retention.

The Young's modulus is the resistance of a material to elastically deform under a load. The Young's modulus therefore directly expresses the elasticity of a material (to reversibly deform under a load) as well as the stiffness or resistance of such a material (to oppose to the elastic deformation under a load). For this reason, sometimes the terms "elasticity", "stiffness" and "resistance" are used interchangeably in corneal studies. A higher Young's modulus of a bioengineered corneal stroma, for instance, indicates a stiffer construct that less easily deforms under a load. For the cornea, the Young's modulus varies widely from study to study, ranging between 0.1 and 57 MPa with significant variations based on the region of the stroma characterized, donor age, storage period and measurement method applied.[38] For instance, in a study on healthy individuals, the Young's modulus was found being 0.29 ± 0.06 MPa[39] while in another study performed on *ex vivo* corneas, this value was found to be in the range 4.5–9.0 MPa.[40] The anterior region has been found to be on average about 40% stiffer than the posterior region.[41] The value of the corneas' tensile strength (i.e., the force needed for a material to be pulled before it breaks) is more consistently accepted to be about 3.8 MPa.[42]

Although values of these parameters can vary between studies, intrastudy alterations of such values are linked (including being causative factors) to several pathological conditions, such as ectasias (e.g., keratoconus).[15–19] Alterations in mechanical properties of the corneal stroma following corneal surgery are also considered to be risk factors that can induce the development of morphological abnormalities of the cornea with consequent vision loss.[20–24]

While different methods exist to measure such mechanical parameters, the use of these values provide a standardized tool for quantitative interstudy comparisons. Therefore, in this review we focus on the Young's modulus and the ultimate tensile strength to compare existing studies of bioengineered stroma.

In a physiological corneal stroma, suitable mechanical properties not only ensure support, elasticity and protection of the eye, but also contribute to the biomechanical cues necessary for the stromal cells, the keratocytes, to maintain physiological conditions. Similarly, bioengineered corneas with adequate mechanical properties ensure a successful replacement of the damaged tissue and provide biomechanical cues for keratocytes that need to repopulate the construct and trigger the remodeling process (Figure 1). It is well established that cells of all kinds respond to mechanical changes in the ECM, and corneal keratocytes are no exception. The interactions between corneal keratocytes and the ECM is highlighted by various research studies demonstrating that the ECM modulates proliferation, adhesion, differentiation, function and preservation of the morphology of keratocytes, key players for the healing and remodeling of compromised stromal tissue.[43–47] Keratocytes also exhibit durotaxis and mechanosensing, i.e., the migration to stiffer regions of materials.[48,49] Alteration in ECM stiffness can change, for instance, actin stress

fiber production and focal adhesions, as well as alter keratocytes' phenotype.[50,60] Significant differences in keratocyte alignment, morphology and matrix reorganization are observed between anisotropic and isotropic environments.[51–57] The altered biological and mechanical cues present in an injured stroma are responsible for the keratocyte-to-(myo)fibroblast transition that can potentially lead to uncontrolled ECM deposition, generation of scar tissue and consequent blindness (Figure 1). Therefore, it is crucial that engineered stromal implants are designed to satisfy the requirements not only of transparency and biocompatibility but also of mechanical characteristics, which is key to their long-term keratocyte compatibility, tissue-functional homeostasis, and clinical use. Additionally, the mechanical properties of a stromal construct must also ensure that the implant is capable of withstanding packaging, handling and suturing in the operating theatre by clinical staff.[54]

3. Overview of Existing Approaches for Designing Corneal Stromal Constructs

Figure 3 presents an Ashby plot of the stromal constructs described by ultimate tensile strength and Young's modulus in studies. While comparing mechanical properties of different materials in one graph may be not straightforward (due to different measurement methods, times, conditions and calculations), Figure 3a shows the large variety of the mechanical properties exhibited by a number of materials, some of which are relevant for corneal applications. Other human tissues and materials are included as a point of reference for researchers from the engineering, biology and medical communities. Figure 3b demonstrates that the values of ultimate tensile strength and Young's modulus approach those of the physiological human cornea only for a limited number of bioengineered corneal stroma. This, in part, is due to the wide range of properties presented by biocompatible technical materials used, such as polymers and metals (Figure 3a). Although a direct comparison of single reports may be challenging, the plot in Figure 3b provides a general landscape of the mechanical properties exhibited by existing bioengineering approaches for stromal constructs. Direct comparison can also be challenging because of different testing instrumentations used among laboratories. Most labs make use of universal mechanical testing machines (with a variety of load cells) to characterize Young's modulus and ultimate tensile strength, however this quantification can also be performed using atomic force microscopy (AFM), nanoindenters, and rheometers. In addition, interpretation of often nonlinear and viscoelastic material properties is not straightforward and can be handled differently among labs. Such differences result in a relatively wide range of values of mechanical properties for the cornea, in particular regarding the Young's modulus, whose extent is illustrated in Figure 3b by a dashed-line circle, labeled "human cornea extended range." Nevertheless, in order to simplify comparisons amongst studies, a restricted range of values for the Young's modulus (indicated in Figure 3b with a continuous-line circle) can be extrapolated from studies that provide both biomechanical characterization of their bioengineered stromal implants and references values for the human cornea. The range of values for the Young's modulus of the human cornea among these studies is more consistently reported to be between 3 and 13 MPa.[24,55–61]

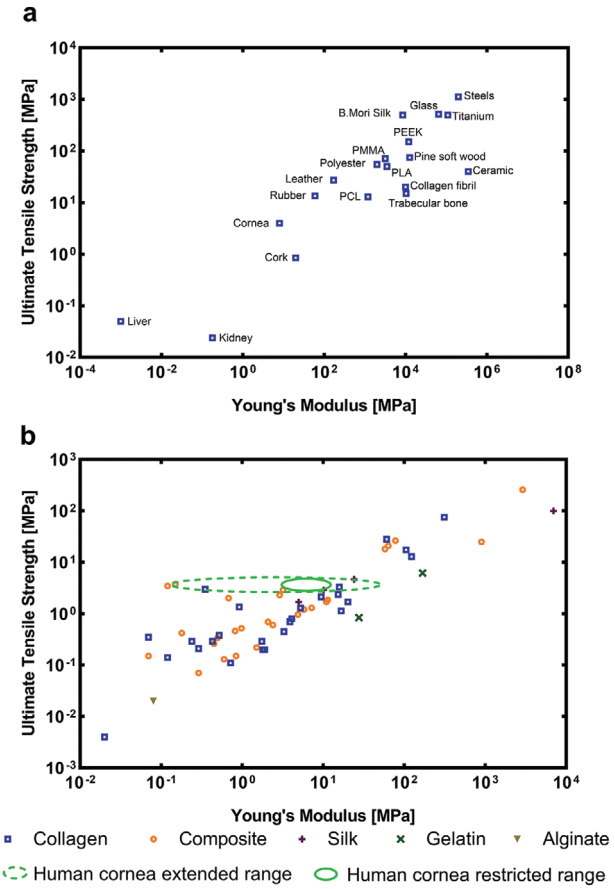

Figure 3. a) Ashby plot of the Young's modulus and ultimate tensile strength showing mechanical characteristics of human tissues including the cornea in comparison to some polymers used in ophthalmic applications and other commonly known materials. b) Ashby plot showing the mechanical properties of the human cornea compared to corneal constructs. The dashed-line circle includes a wider range of values reported in literature for the Young's modulus of the cornea, while the continuous-line circle illustrates a more consistently reported range of values, which is in agreement with most of the studies that present bioengineered stromal implants in this review.

In Figure 3, and in Sections 3.1–3.3, we review only those studies that have considered the need for mechanical characterization and stabilization and who provide a quantitative assessment. These corresponding implants differ by their (combination of) materials and manufacturing methods. The approaches they are based on range from compaction and cross-linking of collagen to the use of composite materials, from the optimization of scaffold architecture to the inclusion of decellularized extracellular matrix (dECM) (**Figure 4**). It is worth noting that classification of the approaches purely based on material composition is not always straightforward. In particular, a substantial number of studies are based on blends of different materials, oftentimes reported as composite materials. This has allowed scientists to combine, for instance, the tailored properties of lab-made (synthetic) materials with biological properties of natural materials. However, since in the vast majority of cases synthetic materials are not used alone to bioengineer stromal constructs, they do not form a separate group of approaches in this review. **Table 1** reports a summary

Table 1. Summary of stromal constructs that report on the quantification of the corresponding mechanical properties. Where in vivo work has been performed, this is discussed in the text.

Material	Method	Key mechanical property		Ref.
Collagen–chitosan	1-ethyl-3-(3-dimethylaminopropyl) carbodiimide/*N*-hydroxysuccinimide crosslinking	Ultimate stress [MPa]	0.145	[62]
		Ultimate elongation [%]	39	
		Young's modulus [MPa]	0.838	
		Toughness [MPa]	0.0188	
	Poly(ethylene glycol) dibutyraldehyde and 1-ethyl-3-(3-dimethylaminopropyl) carbodiimide/*N*-hydroxysuccinimide hybrid crosslinking	Ultimate stress [MPa]	0.220	
		Ultimate elongation [%]	45	
		Young's modulus [MPa]	1.5	
		Toughness [MPa]	0.025	
Collagen	1-ethyl-3-(3-dimethylaminopropyl) carbodiimide/*N*-hydroxysuccinimide crosslinking	Young's modulus [MPa]	1.75	[57]
		Elongation at break [%]	20.1	
		Tensile strength [MPa]	0.286	
Collagen	Polyrotaxane multiple aldehyde crosslinking	Suture resistance [N]	0.46	[63]
		Elongation at break [%]	31	
		Young's modulus [MPa]	1.59	
	1-ethyl-3-(3-dimethylaminopropyl) carbodiimide/*N*-hydroxysuccinimide crosslinking	Suture resistance [N]	0.23	
		Elongation at break [%]	20	
		Young's modulus [MPa]	1.17	
Collagen	Polypropylene octamine crosslinking	Young's modulus [MPa]	1.4	[64]
		Strength [N]	1.2	
		Suture strength [g]	5.5	
Collagen	Strain-promoted azide-alkyne cycloaddition	Storage modulus [MPa]	4.24×10^{-5}–1.12×10^{-1}	[65]
Collagen-glycosaminoglycan	Dehydrothermal treatment	Compression modulus [MPa]	$0.5 \times 10^{-3} - 1 \times 10^{-3}$	[66]
		Tensile modulus [MPa]	1.96×10^{-3}–7.46×10^{-3}	
Deepithelialized cornea	Rose bengal crosslinking	Stiffness [N·mm^{-1}]	1.49–2.92	[67]
		Young's modulus [MPa]	6.86–16.3	
		Ultimate tensile strength [MPa]	1.35	[68]
		Young's modulus [MPa]	0.924	
Collagen–gelatin–hyaluronic acid	Collagen composite	Ultimate tensile strength [MPa]	18.2–26.2	[69]
		Elongation at break [%]	31.3–33.5	
		Young's modulus [MPa]	58–78	
Collagen–phosphorylcholine	Collagen composite	Tensile strength [MPa]	1.29–2.37	[58]
		Elongation at break [%]	38–28	
		Young's modulus [MPa]	5.26–15.3	
Collagen–dialdehyde cellulose nanocrystal	Collagen composite	Young's modulus [MPa]	900	[24]
		Break stress [MPa]	25–33	
		Break strain [%]	5–9	
Polyvinyl acetate-collagen	Electrospinning	Tensile strength [MPa]	0.86–3.6	[70]
Polycaprolactone–collagen	Electrospinning	Toughness [N·m^{-1}]	97–372	[71]
		Elasticity [MPa]	11–13	
Silk	Spin-assisted layer by layer assembly	Young's modulus [MPa]	3.1×10^3–8.6×10^3	[72]
		Ultimate tensile strength [MPa]	10–30	
Silk	Multilamellar film stacking	Young's modulus [MPa]	5.00–24.2	[40]
		Ultimate tensile strength [MPa]	1.68–4.66	
Silk	Centrifugal casting	Young's modulus [MPa]	43.2	[73]
Silk-chitosan	Blend film	Tensile strength [MPa]	0.9–1.3	[74]

(*Continued*)

Table 1. Continued.

Material	Method	Key mechanical property		Ref.
Silk-poly(*l*-lactic acid-*co*-ϵ-caprolactone)	Electrospinning	Tensile strength [MPa]	1.90–9.39	[75]
Silk	Riboflaving and retionic acid crosslinking	Young's modulus [MPa]	350–525	[76]
Silk – tropoelastin	Blend film	Ultimate tensile strength [MPa]	0.68–11	[77]
		Young's modulus [MPa]	0.6–2	
Collagen – silk	1-ethyl-3-(3-dimethylaminopropyl) carbodiimide/*N*-hydroxysuccinimide crosslinking	Tensile stress [MPa]	0.8–1.2	[78]
		Young's modulus [MPa]	4.5–6	
		Elongation at break [%]	20–40	
Fish scale collagen	—	Tensile strength [MPa]	9.76	[79]
		Elongation at break [%]	9.44	
		Tearing strength [N]	2.31	
Fish scale collagen	—	Young's modulus [MPa]	11.7	[80]
Fish scale collagen	—	Young's modulus [MPa]	273–613	[81]
Gelatin–alginate	Electrospinning	Tensile Young's modulus [MPa]	0.45–0.50	[82]
		Elongation at break [%]	63 – 64	
Gelatin–alginate	Electrospinning	Young's modulus [MPa]	3.21	[83]
		Tensile strength [MPa]	2.94	
Gelatin	Ascorbic acid addition	Young's modulus [MPa]	14.0–16.3	[84]
Gelatin–chondroitin sulfate	1-ethyl-3-(3-dimethylaminopropyl) carbodiimide crosslinking	Young's modulus [MPa]	5.3–8.5	[85]
Gelatin–chondroitin sulfate	1-ethyl-3-(3-dimethylaminopropyl) carbodiimide/N-hydroxysuccinimide crosslinking	Young's modulus [MPa]	3.4–8.4	[86]
Gelatin and polycaprolactone	Electrospinning and glutaraldehyde crosslinking	Tensile modulus [MPa]	$15–1.9 \times 10^3$	[87]
		Elongation at break [$mm \cdot mm^{-1}$]	0.014–0.229	
Gelatin–collagen	1-ethyl-3-(3-dimethylaminopropyl) carbodiimide/*N*-hydroxysuccinimide crosslinking	Young's modulus [MPa]	3.92×10^{-3}–6.28×10^{-3}	[55]
		Complex modulus [MPa]	1.32×10^{-3}–2.23×10^{-3}	
		Loss tangent:	0.049–0.061	
Gelatin methacrylate	Poly (ϵ-caprolactone)-poly (ethylene glycol) fiber reinforcement	Maximum tensile strength [MPa]	3.47–3.79	[25]
		Compressive modulus [MPa]	0.120–0.155	
Keratocyte loaded gelatin methacrylate hydrogel	3D printing	Compressive modulus [MPa]	0.01–0.02	[88]
Poly(vinyl alcohol) hydrogel	Cellulose reinforcement	Stress to failure [MPa]	0.15	[89]
		Strain to failure [%]	383	
		Toe point modulus [MPa]	0.160	
		Young's modulus [MPa]	0.071	
Poly(ethylene glycol) dimethacrylate hydrogel	Cellulose reinforcement	Elastic shear modulus [MPa]	8.80×10^{-3}–46.3×10^{-3}	[90]
		Young's modulus [MPa]	0.060–0.30	
		Failure stress [MPa]	0.200–0.650	
		Failure strain [%]	65–95	
Rabbit cornea	Carbon nanotube injection	Young's modulus [MPa]	11.8–13.0	[91]
		Yield stress [MPa]	1.9–2.3	
		Failure strain [%]	0.41–0.47	
Gelatin–alginate	Electrospinning	Young's modulus [MPa]	0.50–0.98	[92]
		Strength [MPa]	0.34–0.52	
Collagen	Peptide amphiphile coating	Young's modulus [MPa]	26–46	[93]
Beta cyclodextrin-mediated collagen – porcine small intestinal submucosa	Composite	Young's modulus [MPa]	2.5–7.5	[94]
		Strain at break [MPa]	5	

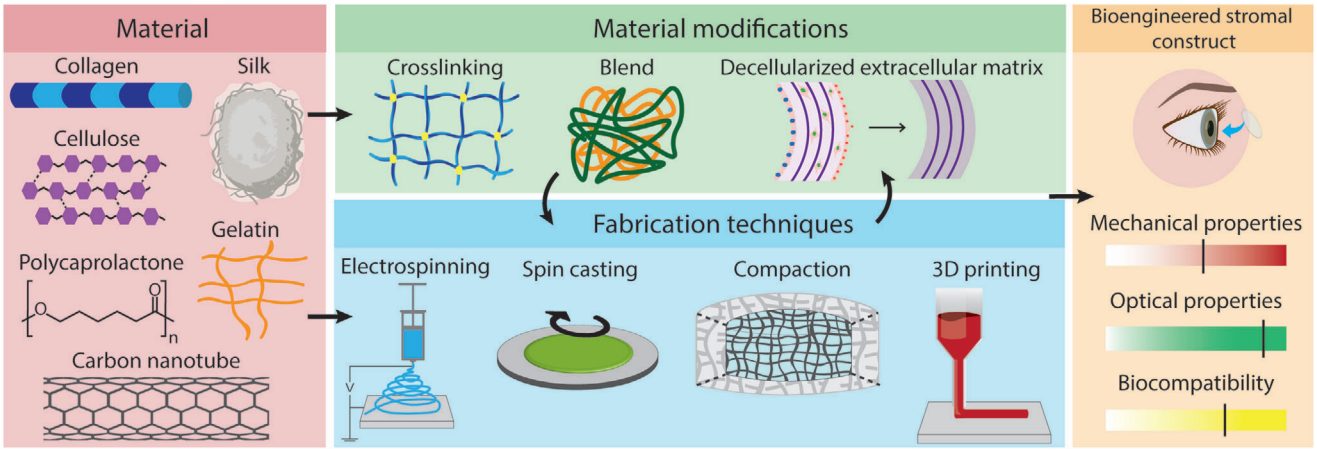

Figure 4. Examples of common materials, material modifications, and fabrication techniques that are used for the engineering of stromal constructs. Together, these should contribute to a stromal construct with sufficient mechanical properties, optical properties and biocompatibility.

of the corneal constructs reported in this review, which is not intended as an exhaustive collection of all the studies on the field but of those for which quantification of mechanical properties was provided.

When trying to mimic the native human stroma, collagen is an obvious choice.[13] While collagen is the main stromal constituent, there are limitations to this approach. Animal-derived collagen constitutes the source of the majority of these studies, however, its possible use in humans can induce immunogenicity risk.[95] The use of low-density collagen materials impacts on the final biomechanical environment of the construct. Difficulties obtaining high-density collagenous solutions is an obstacle to its adoption as raw starting material for biomedical applications.[96] This limitation has driven the search for fabrication processes aimed at improving mechanical characteristics of low-density collagen in its dry state, which could be retained upon hydration. This is achieved either by removing water content to increase collagen density or by strengthening the bonds and architecture of collagen fibrils.

Compaction/compression of collagen removes water and improves mechanical stability. However, cell infiltration is hampered, which complicates long-term implant integration. Integration of cells prior to implantation is possible,[97–99] but is complicated by the (non-)maintenance of keratocyte phenotype in vitro. Collagen cross-linking increases stiffness and tensile stress, however, it comes with a reduced biocompatibility and possible toxicity of remnant cross-linking agents.[100–102] For these types of solutions, the main challenge is finding a reasonable balance between mechanostability and biocompatibility during the first months after implantation, so that residing keratocytes are able to effectively re-establish a healthy ECM.

To overcome the limitations of collagen-only solutions, alternative approaches are based on the use of additional compounds and fabrication techniques. By using composite materials, one can reduce the need for high concentrations of animal derived collagen, improve biomechanical properties, alter biodegradation profiles and influence biocompatibility and growth. As an alternative to collagen, gelatin is easily available, biocompatible and affordable.[103] However, in addition to also being animal-derived, gelatin itself is considerably weaker than collagen and degrades relatively fast. Thus, the desired biomechanical properties can be reached only if the material is cross-linked and/or combined with additional compounds. While current overall biomechanical performances lag behind optimal values, the gelatin methacrylate (GelMA) blend provides an interesting approach for cell preloading prior to cross-linking, which positively impacts both transparency and mechanical properties.[25,88,104]

Fish scale is also an interesting approach to obtaining collagen in large volumes, and while its ultimate tensile strength may be compatible with the human cornea, elasticity needs further improvement.[79,80]

Inclusion of dECM may overcome the problems of animal-derived biomaterials. dECM can be obtained from cornea or from other organs of the human body and in incorporated in constructs, generally improving biocompatibility. Corneal lenticules provide a particularly promising source of corneal dECM, obtained from the tissue excised during small incision lenticule extraction (SMILE) surgery for myopia/astigmatism.[105] However, mechanical properties are not always improved.[106] Whether this is due to the nature of the dECM or the method of its incorporation resulting in nonhomogenous construct or hydration, further work is required to establish the best method of making use of dECM and its abilities to influence keratocytes. Additional limitations of dECM include potential immunogenicity induced by incomplete decellularization, low reproducibility due to donor variability and donor shortages.

Reinforcement can also be achieved by using fabrication techniques that allow researchers to (partially) control the intrinsic architecture of the components of the implant. In this way, silk can be used for corneal constructs. Silk offers control over its mechanical properties by varying the biofabrication process used and therefore can potentially target the optimal biomechanics of the native cornea. Moreover, silks' degradation rates can facilitate the native ECM replacement process upon implantation.[107] However, silk implants present the issue that transparency decreases with increasing thickness, impacting translatability to clinic.[110]

Other fabrication techniques to allow control over anisotropy include electrospinning, extrusion and three-dimensional (3D) printing. Electrospinning can be used to produce supporting meshes that confer increased strength, elasticity and suture retention. However, the process of electrospinning collagen can potentially degrade the collagen triple helix structure.[108,109] For this reason, electrospinning is usually employed with materials such as polycaprolactone (PCL), polyvinyl alcohol (PVA) or poly(lactic-*co*-glycolic acid) (PLGA) to produce meshes to support collagen or other materials. In addition, electrospun constructs can produce a reduced overall transparency, and fiber size and alignment must be tightly controlled to reduce scatter and allow suitable light transmission. Extrusion[110,111] and 3D printing[88] have shown promising results for other applications, but are yet to be fully explored for stromal engineering. One common issue for these techniques is the loss of transparency due to the creation of rough interfaces between layers of extruded/bioprinted products; however, with advancing technology allowing further increases in resolution, they may prove helpful for the engineering of corneal tissues. A more in-depth description of all these different approaches (and their respective mechanical performances) is reported in Sections 3.1–3.3.

3.1. Collagen for Engineering Corneal Stromal Constructs

As the native human stroma mainly consists of collagen type I, a collagen-based implant can provide some of the key features of the in vivo environment.[13] Collagenous materials can be processed in a wide range of ways, creating films, sponges, hydrogels, or fibers that can provide some support for keratocyte survival and function.[37,112,113] Additionally, collagenous materials demonstrate biodegradation over time.[55,114]

Most collagens utilized in vitro are extracted from animal sources such as rats, cows, fish, chickens, rabbits and humans. During the extraction process, the secondary structure of collagen is broken down by the removal of cross-links, resulting in disassembly of the native collagen fibrillary structure into individual monomers.[96] Since monomers spontaneously self-organize into homo- or heterotrimers over time, acetic acid is commonly used to reduce the pH of storage solutions and keep the collagen in a monomeric state.[115] Upon adjusting the pH, temperature and concentration of the monomeric solution, material properties, such as density, pore size, fibril diameter and water content, can be tuned during the self-assembly process, resulting in highly customizable environments for biomedical applications. However, obtaining engineered collagen constructs with properties matching stromal tissue in vivo (e.g., concerning fiber thickness, alignment and spacing) is challenging. As a result, mechanical properties of collagenous engineered constructs rarely match those of the stromal layer in vivo. In order to improve the mechanical properties of in vitro-engineered collagenous constructs, a variety of methods have been proposed and tested. Inspired by the natural process of collagen fibrillogenesis, cross-linking has been studied extensively. Collagen compression, the formation of composite materials and decellularized native stroma are also promising avenues that can lead to the development of collagen-containing stromal constructs with adequate mechanical properties.

3.1.1. Collagen Cross-Linking

A well-studied strategy to reinforce collagen containing constructs is by cross-linking the materials using chemical (e.g., using aldehydes, genipin or carbodiimides), physical (e.g., dehydrothermal or ultraviolet (UV) light) or enzymatic (e.g., transglutaminase) cross-linking.[116–118] in vivo, cross-linking is realized by the formation of covalent bonds both between and within collagen fibrils. These cross-links are enabled by the enzyme lysyl oxidase, and result in increased material stiffness and a reduced chance of microfibrils unravelling.[96,119] Enzymatic cross-linking is widely observed in vivo, and efforts have been made to investigate the potential of enzymatic cross-linking for corneal engineering. Studies utilizing transglutaminase as a cross-linker for in vitro collagenous constructs showed promising results, but the in vivo application has been limited to cross-linking of corneal collagen in rabbits so far.[120–123]

A commonly used strategy for cross-linking collagenous constructs is via chemical means, which are known to increase the breaking strength and stiffness of the collagen fibers while also drastically raising their denaturation temperature. By mixing water-soluble cross-linking agents with other constituents and pouring into a mould, stromal-shaped constructs can be manufactured. Glutaraldehyde is a popular chemical cross-linker due to its ease of use and affordability, but residual glutaraldehyde has been shown to cause calcification and mutagenesis and be cytotoxic. Hence, it is not ideal for the production of engineered corneal implants.[100,101] An alternative is genipin, a chemical cross-linker of natural origin that can form both inter- and intramolecular cross-links in collagen fibrils. in vitro, genipin has shown to be a successful cross-linker in collagen type I hydrogels, increasing storage and loss moduli by a factor of 15 and 4.5, respectively.[102,124] However, some studies have also shown that genipin exhibited low levels of dose-dependent cytotoxicity.[102] When tested on dissected corneas, cytotoxicity induced by genipin cross-linking seemed to be comparable to that of UV-based methods.[125,126]

In an attempt to address the issue of cross-linker toxicity, chemicals that are not directly incorporated into the collagen matrix may be used. Ethyl-3(3-dimethylamino)propyl carbodiimide (EDC) in combination with *N*-hydroxysuccinimide (NHS) leads to amide and ester bond formation between activated carboxyl and amine groups or carboxyl and hydroxyl groups, respectively.[127] Rafat *et al.* showed an improvement in tensile strength and Young's modulus upon increasing the molar ratio of EDC/NHS in their collagen type I scaffolds.[62] Other types of collagen can also be cross-linked using EDC/NHS chemistry. The chemical reinforcement of recombinant human collagen type I and III resulted in stable collagen constructs, sometimes even with higher Young's moduli (17–20 MPa) compared to human corneas (3.0–13 MPa).[56,57,61,128] Although the higher Young's moduli of EDC/NHS cross-linked constructs are an interesting outcome of several studies, methodological inconsistency has led to variable results.[129] The amount of EDC and NHS relative to the available amine groups in the construct has been found to influence the final mechanical properties and biological performance.[62,117] The decrease in biological performance by the increasing amount of EDC/NHS is a logical consequence as both cells and the

cross-linker utilize the same primary amine groups available on the collagen.[130]

A variety of other cross-linkers have been used to improve the mechanical properties of collagen-containing constructs. Lei *et al.* showed that chemical cross-linking based on polyrotaxane multiple aldehydes (PRA) improved suture resistance, elongation at break, storage/loss modulus, and demonstrated acceptable optical properties.[63] Here, the Young's modulus of PRA cross-linked collagen was 1.6 MPa, compared to 1.2 MPa for EDC cross-linked collagen. Additionally, cross-linkers such as polypropylene octamine dendrimers, or methods based on modified collagen molecules show great promise in strengthening engineered constructs.[64,65] Dendrimer cross-linked collagen even showed a Young's modulus of 1.4 MPa, at least one order of magnitude higher compared to glutaraldehyde and EDC cross-linked collagen in the same study.

Physical cross-linking is also used for the fabrication of engineered stromal constructs. Dehydrothermal (DHT) treatment has been shown to enhance collagen containing materials.[66] Crabb and Hubel compared DHT treatment with glucose-mediated UV treatment on collagen and observed a significantly lower relaxation modulus when treated with DHT.[131] UV-cross-linking is also a promising strategy for the reinforcement of in vitro constructs. Both glucose-mediated UV treatment and UV irradiation in combination with a photosensitizer such as riboflavin (vitamin B_2) are known to form intra- and interfibrillar carbonyl-based cross-links.[132] The latter is mainly used for the cross-linking of in vivo collagen in corneal-ectatic patients, but has also been shown to enhance the Young's modulus of hydrogels from 6.8 to 25 kPa in vitro.[106] Riboflavin-mediated UV-irradiation however is cytotoxic to keratocytes in vivo.[67] For clinical use, rose bengal in combination with green light (RGX) appears to result in significantly less cell death and improved mechanical reinforcement.[67,133]

3.1.2. Collagen Compression

One of the shortcomings of using extracted (animal) collagens for the formation of biomaterials in vitro is the relatively low concentration that is obtained after purification.[96] This generally leads to engineered constructs with lower amounts of collagen compared to in vivo tissues. In order to overcome this limitation, compression methods reducing the construct volume (mostly in hydrogel form) have been developed. Via mechanical (application of weight) or electrochemical (application of an electric field) compression, the density of collagen gels is greatly increased and water removed, resulting in thinner constructs that are favourable for light transmittance.[114] However, as density increases in compressed matrices, pore size decreases, potentially limiting cell infiltration and migration. For this reason, cells are often included in the collagen constructs before compaction.[97,98,114]

Besides improved optical properties, collagen compaction also alters the mechanical properties of constructs. Cheema *et al.* showed that an increased collagen fiber density leads to an increase in Young's modulus from 1.1 to 2.3 MPa.[134] Compressed collagen constructs studied by Drechsler *et al.* exhibit values of Young's modulus even superior to those of conjunctiva or amniotic membranes, both materials used in the clinic (0.9, 0.067, and 0.35 MPa for the compressed collagen, conjunctiva and amniotic membrane, respectively).[68] When compared to stromal tissue however, compressed collagen gels still lack stiffness as well as tensile strength.[135]

Although mechanical properties of compressed collagen matrices do not meet in vivo values, constructs still appear suited for the use in clinical settings, as constructs are able to withstand handling during surgery.[68] Initial in vivo data shows potential for the transplantation of compressed collagen matrices in both human and rabbits.[136,137]

3.1.3. Collagen Composites

An alternative approach to reinforce collagenous constructs is the formation of collagen composites, often using biocompatible, Food and Drug Administration (FDA)-approved polymers such as PCL, PVA, or PLGA.[70,71,114,138] Hydrogels can also be made from combinations of materials. In a study by Liu *et al.*, hyaluronic acid (HA) is added to a collagen-gelatin composite hydrogel. Using the collagen-gelatin-HA mix with varying mass ratios of HA, it was shown that the introduction of HA increases both the tensile strength and Young's modulus significantly.[69] The same holds for collagen–chitosan hydrogels, where the addition of chitosan improved the ultimate stress, ultimate elongation, stiffness, and toughness. This approach suggests great potential in terms of both physical and biological performance as the construct withstood long-term in vivo implantation.[62] In the 12-month postoperative study, the cornea construct was implanted in pig eyes and showed to be cell friendly, strong, elastic, bioresorbable and superior to human eye bank corneas in optical clarity. A third composite approach that demonstrated favourable in vivo results contained 2-methacryloyloxyethyl phosphorylcholine (MPC). MPC was combined with collagen to create an interpenetrating polymeric network.[58,128] Interestingly, the mechanical influence of MPC on collagen appeared to be species-specific.[128] The stiffness and tensile strength of porcine collagen hydrogels increased significantly from 0.60 to 2.1 MPa and 0.13 to 0.69 MPa, respectively, when combined with MPC. For recombinant human collagen type III gels however, the stiffness decreased from 20 to 5.3 MPa upon addition of MPC. Also, a change in ultimate tensile strength was noted, as addition of MPC led to a respective reduction from 1.7 to 1.3 MPa.

Dialdehyde cellulose nanocrystals (DAC) have shown to be a promising material that can be used to reinforce hydrogel constructs for ocular use. An increase in DAC concentration results in an increase in water content and mechanical properties. The composite material shows potential as a drug delivery system, however, a downside of the addition of DAC is decreased optical performance.[24]

3.1.4. Collagen Electrospinning

Electrospinning is a popular method of producing biphasic or blended scaffolds of collagen reinforced by polymers. Electrospinning shows great potential for both aligning cells with respect to the scaffold fibers and ensuring that the transition from corneal fibroblasts to myofibroblast phenotype is reduced.[139]

However, most studies overlooked the mechanical characterization to demonstrate whether the scaffolds are stable enough for clinical use.[140,141]

Addition of electrospun polymers to collagen gels may be used to improve the suturability of constructs. Compared to collagen only, the tensile strength of collagen-electrospun PCL membranes was higher, and demonstrated improved suture retention in engineered suture pull-out tests. Additionally, keratocytes were able to proliferate and align in the direction of the collagen fibers for up to 4 weeks.[114] Wu *et al.* demonstrated that the addition of PVA to electrospun collagen increased Young's modulus, alongside an increase in tensile strength from 0.86 MPa for 7% aligned PVA-collagen, to 2.3 MPa for 9% nonaligned collagen and 3.6 MPa for 9% aligned PVA-collagen. That means that with aligned electrospun scaffolds a tensile strength similar to that of the natural tissue can be obtained.[70] Kim *et al.* manufactured an advanced dome-shaped electrospun scaffold with radially aligned collagen-PCL fibers,[71] providing a favorable environment for cells and optical properties that minimized light scattering. Besides, the Young's modulus of the radially aligned construct was 13 MPa, similar to that of the human cornea.

Collagen hydrogels reinforced by aligned PLGA electrospun fibers also have been used as a strategy to match both biological and mechanical requirements of the native tissues. The stiffness and maximum tensile stress were both shown to match the mechanical performance of the natural corneal tissue, while meeting the requirements for optical transparency.[138]

It should be noted that while electrospinning is a key technique for introducing controllable fiber environments and anisotropy to corneal constructs, the process of electrospinning collagen using fluoroalcohols as solvents (e.g., 1,1,1,3,3,3-hexafluoro-2-propanol (HFIP) or 2,2,2-trifluoroethanol (TFE)) is thought to denature the collagen triple-helix structure.[108,109] However, researchers have reported that electrospinning in benign solutions maintains the triple helix,[142,143] and that the effect of electrospinning on collagen is still unknown.[144] Further research is needed to investigate the relevant parameters that are responsible for the denaturation of the natural structure of collagen during electrospinning.[145]

3.2. Alternative Materials for Bioengineering Stromal Constructs

While collagen possesses some of the biological and mechanical features necessary for a stromal construct, hurdles such as bioengineering fully native-like collagen fibers, obtaining high concentrations and enhancing its mechanical strength led researchers to investigate alternative natural materials. Materials used for stromal constructs include amniotic membrane, silk fibroin, fish scale and natural polymers, such as gelatin, alginate, cellulose, chitosan, fibrin and HA. Such materials are chosen for their favorable biological properties; they are biocompatible, degrade in a nonharmful manner, enable cell attachment and allow biofunctionalization.[146] However, in some instances, these materials underperform biomechanically. To achieve preferred biomechanical performances and architectures, natural materials are often combined with synthetic polymers to form composite constructs. In this section, we will focus on materials whose mechanical properties can be tuned by combination with supportive materials to meet the biomechanical requirements of a corneal implant.

3.2.1. Silk

Silk and its derivative, silk fibroin, is derived from the cocoons of *Bombyx mori, Antheraea pernyi*, and *Antheraea mylitta* worms, and is produced in high volumes for low costs. Silk fibroin protein became popular for ophthalmologic applications due to its biocompatibility, biodegradation and high mechanical strength.[147] Although it can be easily fabricated in various forms and thicknesses, its transparency decreases drastically with increasing thickness and therefore it is not generally suitable to be used alone for the replacement of large parts of the corneal stroma.[110] Nevertheless, silk fibroin also has the advantage of degrading slowly and predictably in the cornea (typically over several weeks), and thus provides the time keratocytes require to produce their own ECM within the construct.[148]

Despite the limitation on the thickness, silk fibroin can provide high mechanical strength also when produced as thin films. For instance, Jiang and co-workers demonstrated that silk fibroin films 20–500 nm thick exhibit excellent mechanical strength.[72] Such ultrathin films were produced by spin coating or spin-assisted layer-by-layer assembly, resulting in an enrichment of the β-sheet crystalline structures within the silk films. These β-sheets serve as physical cross-links, producing a Young's modulus of 6–8 GPa and ultimate tensile strength of 10 MPa. For stromal applications however, their poor elasticity (< 3%, i.e., up to tenfold lower than for bulk silk[149]) and their ultrathin thickness (unless methods for stacking multiple films are implemented) can be limiting factors. With such limitations in mind, researchers are working on producing thicker silk structures. Ghezzi and colleagues developed a strategy based on stacks of orthogonally oriented films to obtain 3D silk structures.[40] Recapitulating the structures of lamellae in the native stroma, the construct was assembled and cultured with corneal cells over a period of 9 weeks. To aid cell attachment and alignment, individual films were patterned with microgrooves and were arginine-glycine-aspartate (RGD)-functionalized. The authors also claimed that the integration of stromal cells producing own collagen further improved the cohesiveness, transparency and mechanical properties of the construct. The 3D silk construct alone showed a Young's modulus and ultimate tensile strength of 10 and 2.9 MPa, respectively. These values changed to 5.0 and 1.7 MPa when human corneal fibroblasts were added to the construct and to 24 and 4.7 MPa when human corneal stromal cells were added.

To tackle the issue of poor elasticity and transparency deriving from conventional dry casting silk manufacturing procedures, Lee *et al.* proposed centrifugation as an alternative strategy to produce silk films.[73] This approach not only increased mechanical properties, including elasticity and transparency but also resulted in smoother surfaces and improved keratocyte proliferation. Surprisingly, a 50 μm thick film had a higher tensile strength than both 20 and 80 μm thick films. Young's modulus for centrifugal casting was 43 MPa, ≈34% more than for dry casting.

Increased transparency and phenotypic keratocyte behaviour could be achieved also by addition of additional materials to silk. For instance, Guan *et al.* explored the effect of silk fibroin functionalization with varying amount of chitosan.[74] While the scaffolds showed an improved keratocyte morphology and marker expression, the tensile strength was in the range of 0.9–1.3 MPa, lower than for native corneas. Biodegradation of the composite scaffolds took 3–4 months. Overall, as demonstrated in several other studies,[62,89] chitosan improves biological and degradation properties rather than mechanical properties. Another interesting application used for enhancing the mechanical properties of silk constructs, although tested so far only for the culture of endothelial cells, is the integration of poly(*l*-lactic acid-*co*-ϵ-caprolactone) (P(LLA-CL)) electrospun fibers.[75] In this study, Chen and co-workers tested different ratios of silk to P(LLA-CL), with the ratio 25:75 demonstrating highest optical transparency. The construct was 56 μm thick and for this ratio the tensile strength increased from 1.9 (silk alone) to 9.3 MPa.

Riboflavin and retinoic acid have also been used in silk fibroin matrices in a recent study by Bhattacharjee *et al.* as a strategy to improve both mechanical properties and cell phenotype.[76] To demonstrate this, using 20×10^{-3} M riboflavin as a photocrosslinker led to an increase in Young's modulus from ≈350 to 525 MPa for 35 μm thick films. To achieve elasticity values that are closer to native adult stromal tissues, tropoelastin has also been investigated as an additional compound to pure silk structures.[77] Films were produced with thickness between 28 and 94 μm and by altering the tropoelastin-to-silk ratio, the Young's modulus could be tuned between 0.7 and 11 MPa, while ultimate tensile strength ranged from 0.6 to 2.0 MPa. In this study, the addition of tropoelastin also increased nutrient permeability as well as cell attachment and growth. In addition, in this study by Aghaei-Ghareh-Bolagh, suture retention strength was also tested, showing that although their constructs presented a value of 19.8 g-force, which is less than the value of native cornea (35.7 g-force),[64,150] this was enough to withstand a typical 10-0 nylon suture used in ophthalmic surgery.

By combining silk with collagen, Long *et al.* attempted to increase the strength of a collagen construct while not compromising its high biocompatibility properties.[78] Silk and collagen were mixed at different ratios (1:5, 1:10, and 1:20) and cross-linked by EDC and NHS. Increasing amounts of silk in the collagen produced decreasing values of both the Young's modulus and ultimate tensile strength, while the elongation at break varied in opposite direction. The ratio 1:10 resulted being the best compromise among the different ratios. This composition, having a tensile strength of 0.97 MPa and a Young's modulus of 4.9 MPa, was tested by suturing tests using 10-0 nylon sutures both in vitro and in rabbits as well as for re-epithelialization tests—performing better than the same collagen construct without silk.

3.2.2. Fish Scale

Recently, approaches have been developed using fish scales, mostly from the *Tilapia fish*. These scales are a waste product of the fishing industry and exhibit collagen type I organization and permeability to oxygen similar to that of the human stroma, as well as low immunogenicity.[151,152] Scales can be decellularized, decalcified and then processed with nitric acid to increase the pore size.[153] This simple treatment resulted in constructs with tensile strength between 9.8[79] and 12 MPa,[80] which were demonstrated to be sufficient for successfully suturing the constructs in rats. However, in these attempts to create stromal constructs, localized cracking and shearing could be noticed, indicating that the materials could further benefit from enhancing their elastic properties. In a different study, Feng *et al.* used grass carp scales and added a further etching step to improve light transmittance.[81] Young's modulus of the processed fish scales at different stages (i.e., when collected, decalcified and fully treated) were 610, 390, and 270 MPa, respectively.

3.2.3. Gelatin (and GelMA)

Gelatin has been widely explored for stromal constructs as well as for other corneal applications due to its high compatibility with host tissues and lower cost compared collagen. Gelatin's biological properties stem from the fact that it is derived from the denaturation of collagen, which also allows for easier degradation and reabsorption into the tissues.[25] While these features are desirable for several corneal applications, higher degradation properties translate into weaker mechanical strength. For this reason, gelatin is often reinforced by means of cross-linking and/or combined with other materials to form composites.

In work by Tonsomboon *et al.*, electrospun gelatin fibers were used as reinforcing mats in an alginate hydrogel cross-linked with $CaCl_2$. The authors reported that the higher hydrophilicity of gelatin nanofibers allows increased entrapment of alginate hydrogel compared to PCL electrospun nanofibers.[82] Gelatin-alginate constructs exhibited lower stiffness compared to PCL-alginate. The Gelatin-alginate constructs showed a Young's modulus of 0.5 MPa. This value differed in constructs with aligned or randomly oriented nanofibers. For aligned fibers, the strength increased in the direction parallel to the fiber orientation, while it decreased in the perpendicular direction, therefore randomly aligned gelatin mats were preferred. In a later study, the same author produced improved scaffolds by overlapping several aligned electrospun mats in an orthogonal fashion, reaching values of Young's modulus of 3.2 MPa and tensile strength of 2.9 MPa.[83] By using electrospun nanofibers, the authors claimed that the composite architecture could prevent the propagation of cracks, common in alginate-only hydrogels.

Values of Young's modulus closer to the human eye were obtained in a study by Luo *et al.*, where blends of cryogels, gelatin, and varying amounts of ascorbic acid cross-linked by means of carbodiimide were used as keratocyte carriers.[84] Ascorbic acid was chosen for its antioxidant and cell proliferation properties but was shown to affect the structure and function of the hydrogel. By increasing the concentration of ascorbic acid between 0 and 120 mg mL^{-1} of gelatin, the Young's modulus decreased from 17 to 1.1 MPa, while the degradation rate of the constructs in the presence of matrix metalloproiteinase-1 increased with the amount of ascorbic acid (which in turn decreased the degree of cross-linking and increased the pore dimension).

To improve its mechanical properties, gelatin is often cross-linked using EDC/NHS. Lai and co-workers investigated the

optimal EDC/NHS ratio in gelatin-chondroitin sulfate scaffolds,[85,86] showing that a 2:1 ratio of EDC:NHS allows optimal chondroitin sulfate content for improved biological and transport properties. Varying the NHS-to-EDC ratio produced a decrease in Young's modulus from 8.4 to 4.5 MPa. This decrease in Young's modulus is thought to be related to an increasing amount of chondroitin sulfate and, consequently, water content. EDC/NHS cross-linking was also used in scaffolds made of collagen-gelatin-HA films. Liu and co-workers found that the ratio 6:3:1 of collagen:gelatin:HA films (110 μm thick) with EDC/NHS cross-linking showed optimal overall performance including transparency, diffusion and biocompatibility, with an ultimate tensile strength of 26.2 MPa and a Young's modulus of 78.1 MPa.

Electrospinning of other compounds, such as PCL has also been explored as a strategy to reinforce gelatin.[87] In the dry state, the Young's modulus of gelatin-PCL blends inversely correlates to the amount of PCL, ranging from 136 MPa for only gelatin scaffolds to 15 MPa for only PCL scaffolds. This was reversed for wetted blends and cross-linking with glutaraldehyde did not significantly affect these values for blends that included PCL, both dry and in wet state. Wet scaffolds composed of only noncross-linked gelatin were too fragile to be tested, 100% PCL scaffolds exhibited a Young's modulus of 33 MPa. The ratios 25:75 and 50:50 of gelatin:PCL were chosen for in vitro testing with corneal stromal cells for their overall mechanical and biological properties.

The combination of collagen and gelatin has also been reported as a reinforcement strategy by Goodarzi *et al.*, where the gelatin–collagen blends showed improved mechanical properties with respect to hydrogels made of only gelatin.[55] In this case, blends of gelatin and collagen cross-linked with EDC/NHS produced a Young's modulus of 6.3 MPa, approximately twice the value obtained for scaffolds of only gelatin. The composite scaffolds also possessed increased porosity, which contributed to further support viability and proliferation of human bone marrow mesenchymal stem cells.

Gelatin can be modified with methacrylic anhydride to form GelMA. GelMA hydrogels offer the advantage that they can be mixed with cells prior to rapid photocross-linking with UV light. Kong and co-workers recently demonstrated that GelMA reinforced with a PCL electrospun mesh supported a keratocyte phenotype.[25] In this study, the scaffolds exhibited a tensile strength of 3.5 MPa and compressive modulus of 0.12 MPa. Moreover, the combination of electrospun matrix with GelMA hydrogel facilitated an easier suturing of the construct as demonstrated in in vivo testing.

GelMA can also be 3D-printed together with human keratocytes,[88] and produce values of compressive modulus similar to the human cornea. The same work also demonstrated that preloading GelMA hydrogels with cells improved their optical transparency.[104] The construct made of 15% hydrogel was strong enough to be handled and did not degrade in phosphate buffered saline solutions over 21 days. Cells produced their own collagen, confirming in vivo-like behavior. Although the compressive modulus of 6.5 kPa was significantly lower than for human corneas, the authors claim that the strength of the construct can significantly increase upon culture with keratocytes for 1 month.

3.2.4. Alginate

Alginate is a seaweed-derived material, widely used for biomedical applications, and is particularly popular for forming hydrogels.[154] Its molecular composition can be varied, and the gelation process controlled in order to modify the final properties of the gel. However, due to limited mechanical and cell adhesion properties, alginate is usually mixed with other materials to form composites, coated or modified to improve performance (i.e., with RGD-peptide). In a study by Isaacson and colleagues, alginate was used as a component in several bioprinting inks to create stromal constructs.[155] In such mixtures, alginate improved cell viability, while collagen conferred mechanical strength.

3.2.5. Cellulose

Due to its desirable mechanical properties, bacterial cellulose has been widely explored in recent years for numerous biomedical applications, and is currently used in clinical products for skin.[156,157] Bacterial cellulose is a renewable, affordable and biodegradable natural polymer that has been used to stabilize methacrylate hydrogels.[158] This material offers a high degree of crystallinity and high water holding content, and does not contain harmful plant molecules, such as lignin and hemicellulose. When used at a 2% concentration, in the hydrogels, bacterial cellulose increases the Young's modulus by a factor of 20. Considering its high water storage capacity, bacterial cellulose presents an attractive method of mechanically stabilizing stromal constructs. A similar approach used carboxylated nanocellulose whiskers (CNCs) to stabilize PVA hydrogels[89] for ophthalmic applications. These constructs are transparent and exhibit hyper elastic, rubber-like behavior. The authors consider this due to both high water content and combination of relatively stiff CNCs entangled in a soft polymer matrix of PVA. The constructs exhibit an exceptionally high Young's modulus for a hydrogel; the elastic/storage modulus G' was 16 kPa, and the viscous/loss modulus G'' was 450 Pa. The moduli are well-separated and parallel to each other at the tested frequencies between 1 and 20 Hz, suggesting true viscoelastic solid behavior. In this region, the overall system is characterized by a damping factor δ as low as ≈1.5°, which is remarkable given its water content above 90%. When cytocompatibility was validated using an endothelial cell line, cell expansion, and no toxicity was observed; these results may prove translatable to corneal keratocytes.

Given some preliminary contradictory reports about the biocompatibility of cellulose in the cornea,[159,160] the Zhang group recently assessed the properties of this material for engineering a stromal construct.[161] Although the material did not degrade over a period of 90 days, results confirmed biocompatibility in the eyes of rabbits. Cellulose can be used to reinforce several types of hydrogels. Nanofibrillated cellulose improved the compression modulus, ultimate stress and strain of poly(ethylene glycol) dimethacrylate gels.[90] The compression modulus increased up to 3.5-fold to a maximum value of 300 kPa using a 0.7% volume of nanofibrillated cellulose, while the ultimate stress increased by 180% up to 630 kPa. Additionally, by scattering light in a 3D gel network, nanofibrillated cellulose reduced UV photopolymerization time and therefore the amount of photoinitiator required

for cross-linking. The use of nanofibrillated cellulose also allowed control over the swelling properties of the hydrogels.

3.2.6. Carbon Nanotubes and Graphene

Other researchers have investigated implanting carbon nanotubes into rabbit eyes as a method of strengthening the in situ cornea in progressive diseases where weakening of the stroma is pathogenic.[91] In this study, a saline solution containing carbon nanotubes was administrated by injections in 300 µm deep pockets created by incision from the surface of the cornea. Carbon nanotubes offer potential structural reinforcement due to their high mechanical strength and good biocompatibility. They form aligned core units with collagen shells without using cross-linkers. Furthermore, they have demonstrated strong cell adhesion and protein absorption properties, and were nontoxic in rabbits. These constructs exhibited a maximum Young's modulus of 2.9 GPa (dry) and 2.9 MPa (wet) and break stress of 160 MPa (dry) and 25 MPa (wet). Upon implantation of 1 mg mL^{-1} nanotubes, researchers observed a nonstatistically significant trend toward an increase in Young's modulus of the rabbit corneas from 12.0 ± 2.5 to 13.0 ± 3.9 MPa. Yield stress also increased, although the statistically significant increase to 2.3 ± 0.3 MPa was only observed at the lower nanotube concentration of 0.1 mg mL^{-1}. Although, no interaction between the nanotubes and ECM of the cornea was analyzed in this particular study, prior results from the same group indicated that interaction and adsorption is present between collagen fibers and carbon nanomaterials. These results indicate that the implantation of structural supporting materials such as carbon nanotubes may increase the strength of the cornea and combat pathogenic weakening of the tissue.

Based on the hypothesis that a "skirt support" may be key to providing suitable mechanical stability, researchers applied this concept to hopefully also support cell integration and overcome complications, such as rejection. In this context, the Mehta group has investigated graphene films and foams as potential alternatives to titanium.[162] Graphene has an elasticity index similar to that of rubber, has greater tensile strength than steel, and is harder than diamond, providing ideal characteristics for a skirt support. When primary human stromal fibroblasts were exposed to the graphene film, they demonstrated 10% more proliferation than observed on titanium. Expression of Interleukin-6 and -8 reduced when cells were seeded onto graphene foam and 6 devices were implanted into rabbit eyes with no signs of infection, neovascularization, or inflammation. Although the Mehta group focused on biocompatibility and did not look into the mechanical properties of the graphene constructs used, information from the suppliers show that the film had a tensile strength of 30 MPa.

3.2.7. Decellularized Extracellular Matrices

The addition of dECM components has been explored by Hong *et al*. as a strategy to improve the general performances of collagen gel as bioengineered stroma.[97,98] The use of dECM would carry the additional benefit of providing more physiological biochemical cues. In this respect, the authors concluded that keratocytes cultured within such constructs better represented their optimal quiescent phenotype. Disappointingly, both the tensile strength and the Young's modulus of the hydrogels decreased upon dECM addition and thus are far from sufficient for use in vivo. Mechanical performance even further decreases where only dECM is used, further demonstrating the importance of considering the mechanical impact of incorporating dECM into engineered constructs.[106]

Other groups have taken advantage of dECM to stabilize their constructs. Wang *et al*. 2020 incorporated tissue derived ECM microparticles in a stroma–Bowman's layer dual-environment construct.[163] The ECM microparticle containing layer, derived from porcine small intestine submucosa, exhibited a significantly increased Young's modulus of the dual constructs compared to native cornea by ≈5 MPa, while maintaining optical transparency and cytocompatibility in vivo. Additionally, the incorporation of the ECM microparticle containing layer increased the suturability of the constructs, and when used in rabbits no inflammation was observed 30 days postsurgery.

3.3. Architecture as an Alternative Reinforcement Method

The introduction of tissue architecture can also be considered for reinforcement. in vivo, the layers of the corneal stroma are anisotropically arranged. They contain collagen fibers in two opposing directions, running from the superior to the inferior and temporal to nasal sides of the eyes, mechanically stabilizing the tissue and its shape. Efforts have been made to introduce anisotropy in collagenous engineered constructs, often in combination with fiber reinforcement.[70,71,92] Changes in collagen architecture alone can also alter mechanical properties. In one such study both random and aligned collagenous layers were subjected to AFM stiffness measurements, showing increased stiffness for aligned tissue layers.[93]

Reinforced constructs may also be performed by altering the morphology of hydrogels. Melt electrospinning, extrusion and 3D printing methods can all be employed to pattern biomaterials into specific morphologies using, for example, fibers, filaments and droplets for desired mechanical properties. Melt electrospinning writing was used to produce a "grid" of polycaprolactone to support a soft GelMA hydrogel.[164] Interestingly, this work was led by finite element (FE) analysis of load bearing constructs, capturing both the reinforcement effect of lateral gel expansion and the influence of load transfer through the gel. While this work was not focused on a specific tissue, its in-depth analysis of mechanical behaviour and model-led approach may be an interesting avenue for corneal applications. However the issue of transparency of the grid construct would need to be addressed.

Extrusion of a blend of two polyurethanes [4,40-methylenebis(phenyl isocyanate)-alt-1,4-butanediol/di(propyleneglycol)/polycaprolactone] (polyurethane A) and Texin DP7-1205 aromatic thermoplastic produced a similar grid patterned scaffold with interesting mechanical properties.[126] These grid fibers were used to support an epoxy-based hydrogel. The fracture toughness of these constructs was particularly impressive, and while the authors originally intended the work for cartilage tissue engineering, they may be of interest for improving suturability of other engineered constructs including cornea.

A coextruded polyester fiber-poly(ethylene oxide) (PEO) matrix produced highly tuneable reinforced constructs.[165] By varying the PCL concentration, the hydrogel stiffness could be tailored from 0.69 ± 0.04 to 1.90 ± 0.21 MPa. The influence of fiber orientation and enhanced mechanics via uniaxial drawing of the PCL–PEO composites further increased stiffness by 225%. This work also sought to increase translatability by performing similar experiments with poly(*L*-lactic acid) fiber-reinforced PEO hydrogels with a stiffness of 8.70 ± 0.21 MPa. Cytotoxicity was validated using fibroblast and osteoblast cells—indicating that differentiation pathway could be controlled by tunable mechanical properties. While also not corneal-focused, this demonstrated the potential of reinforcement techniques to not only influence mechanical properties but also cellular response.

4. Conclusion and Future Directions

The need for consideration of the mechanical properties of corneal stromal implants is crucial for their success in a clinical setting. Nevertheless, while most of the studies reporting on bioengineered stroma demonstrate positive results, particularly with regard to biocompatibility, bioengineers are yet to fully appreciate the importance of the biomechanical environment, and the suturability and handleability of otherwise biologically promising constructs. As a consequence, the majority of existing studies either are far from targeting optimal mechanical values or entirely lack biomechanical validation. For the future success of bioengineered stromal constructs further biomechanics awareness is necessary to improve reinforcement techniques. In the first instance, mechanical testing methods are highly variable between studies. To allow true comparison and critique of results, standardized methodology needs to be fully integrated in the assessment of stromal constructs. Additionally, assessment of the mechanical forces applied during corneal suturing is highly heterogeneous. Quantitative measurements are often restricted to suture materials themselves, suture tension,[166] or to suture retention devices for skin, such as the Hemiguard.[167] They also often focus on surgical techniques[168] and are variable between both operator and the tissue in question.[169] Qualitative assessment of novel materials and stromal constructs "handleability" from skilled surgical staff are often relied on by researchers internally, limiting how this data can be extrapolated to other materials and research. Mechatronic surgical robots, such as the Da Vinci, the Sehance and the Robin are of course well characterized for the forces they apply during surgery,[170] but these surgical robots are still rare and in limited use—particularly in developing nations which account for large volumes of corneal transplant need.[171] Clinical assessment of novel bioengineered stromal constructs is limited.[172] Animal trials performed have been discussed throughout this text, with varying degrees of success. The latest stromal constructs on the market, such as the CorNeat KPro, focus on 100% synthetic, nonbiodegradable materials in a similar way to the established Boston KPro. The translatability of other promising materials into clinical trial is perhaps being hampered by this lack of consideration of mechanical characteristics and suturability.

Based on our extensive review of existing literature, composite strategies may be the most promising avenue to a lab-created stromal construct. Such hybrid solutions, combining both engineering and biology to produce mechanically and biologically optimal constructs are desperately needed to address the shortage of donor corneas for patients. Both properties are essential to allow successful integration of the implant, and controlled degradation followed be the natural ECM remodeling process guided by keratocytes. Groups focusing on this hybrid approach are making great strides in this field and continue to produce promising work with the potential to address the donor tissue shortage and restore the sight of patients worldwide.

Acknowledgements

N.F., C.v.d.P., and R.G. contributed equally to this work. Funding sources: This work was supported by the Chemelot InSciTe (project BM3.02).

Conflict of Interest

The authors declare no conflict of interest.

Keywords

bioengineering, corneas, mechanical properties, stromal layers

Received: May 19, 2021
Revised: July 15, 2021
Published online: August 8, 2021

[1] P. Gain, R. Jullienne, Z. He, M. Aldossary, S. Acquart, F. Cognasse, G. Thuret, *JAMA Ophthalmol.* **2016**, *134*, 167.
[2] J. P. Whitcher, M. Srinivasan, M. P. Upadhyay, *Bull.World Health Organ.* **2001**, *79*, 214.
[3] R. Lee, Z. Khoueir, E. Tsikata, J. Chodosh, C. H. Dohlman, T. C. Chen, *Ophthalmology* **2017**, *124*, 27.
[4] L. N. Kanu, M. Niparugs, M. Nonpassopon, F. I. Karas, J. M. De La Cruz, M. S. Cortina, *Ocul. Surf.* **2020**, *18*, 613.
[5] B. E. Malyugin, S. A. Borzenok, M. Y. Gerasimov, *Vestn. Oftal'mol.* **2020**, *136*, 77.
[6] X. Ma, R. Xiang, X. Meng, L. Qin, Y. Wu, L. Tain, Y. Jiang, Y. Huang, L. Wang, *Cornea* **2017**, *36*, 304.
[7] N. Schrage, K. Hille, C. Cursiefen, *Ophthalmologe* **2014**, *111*, 1010.
[8] R. Pineda, *Keratoprostheses and Artificial Corneas: Fundamentals and Surgical Applications*, Springer, Berlin **2015**, pp. 213–219.
[9] V. S. Avadhanam, M. Zarei-Ghanavati, A. S. Bardan, G. Iyer, B. Srinivasan, S. Agarwal, M. Goweida, M. Fukuda, K. Hille, J. Chodosh, C. S. Liu, *Ocul. Surf.* **2019**, *17*, 4.
[10] N. Jirásková, P. Rozsival, M. Burova, M. Kalfertova, *Eye* **2011**, *25*, 1138.
[11] V. Feiz, M. J. Mannis, G. Kandavel, M. McCarthy, L. Izquierdo, M. Eckert, I. R. Schwab, S. Torabian, J. L. Wang, W. Wang, *Trans. Am. Ophthalmol. Soc.* **2001**, *99*, 159.
[12] A. Vannas, B. A. Holden, D. F. Sweeney, *Brit. J. Ophthalmol.* **1987**, *71*, 593.
[13] S. Matthyssen, B. Van Den Bogerd, S. N. Dhubhghaill, C. Koppen, N. Zakaria, *Acta Biomater.* **2018**, *69*, 31.
[14] C. Edmund, *Acta Ophthalmol.* **1988**, *66*, 134.
[15] H. R. Vellara, D. V. Patel, *Clin. Exp. Optom.* **2015**, *98*, 31.
[16] L. A. Carvalho, M. Prado, R. H. Cunha, A. Costa Neto, A. Paranhos Jr., P. Schor, W. Chamon, *Arq. Bras. Oftalmol.* **2009**, *72*, 139.
[17] C. J. Roberts, W. J. Dupps, *J. Cataract Refractive Surg.* **2014**, *40*, 991.

[18] B. J. Blackburn, M. W. Jenkins, A. M. Rollins, W. J. Dupps, *Front. Bioeng. Biotechnol.* **2019**, *7*, 66.
[19] M. W. Belin, R. Ambrósio, *J. Refractive Surg.* **2010**, *26*, 238.
[20] J. B. Randleman, *Curr. Opin. Ophthalmol.* **2006**, *17*, 406.
[21] I. G. Pallikaris, G. D. Kymionis, N. I. Astyrakakis, *J. Cataract Refractive Surgery* **2001**, *27*, 1796.
[22] D. G. Dawson, J. B. Randleman, H. E. Grossniklaus, T. P. O'brien, S. R. Dubovy, I. Schmack, R. D. Stulting, H. F. Edelhauser, *Ophthalmology* **2008**, *115*, 2181.
[23] M. O'keefe, C. Kirwan, *Clin. Exp. Ophthalmol.* **2010**, *38*, 183.
[24] S. Xu, S. Zhou, B. Mao, J. Chen, Z. Zhang, *ACS Sustainable Chem. Eng.* **2019**, *7*, 12248.
[25] B. Kong, Y. Chen, R. Liu, X. Liu, C. Liu, Z. Shao, L. Xiong, X. Liu, W. Sun, S. Mi, *Nat. Commun.* **2020**, *11*, 1.
[26] J. Germundsson, P. Fagerholm, M. Koulikovska, N. S. Lagali, *Invest. Ophthalmol. Visual Sci.* **2012**, *53*, 2354.
[27] P. Català, W. Vermeulen, T. Rademakers, A. van den Bogaerdt, P. J. Kruijt, R. M. M. A. Nuijts, V. L. S. Lapointe, M. M. Dickman, *Cornea* **2020**, *39*, 1407.
[28] M. Mobaraki, R. Abbasi, S. Omidian Vandchali, M. Ghaffari, F. Moztarzadeh, M. Mozafari, *Front. Bioeng. Biotechnol.* **2019**, *7*, 135.
[29] G. Orssengo, *Bull. Math. Biol.* **1999**, *61*, 551.
[30] C. R. Ethier, M. Johnson, J. Ruberti, *Annu. Rev. Biomed. Eng.* **2004**, *6*, 249.
[31] K. Green, L. R. Barge, L. Cheeks, C. I. Phillips, *Acta Ophthalmol.* **1987**, *65*, 538.
[32] H. Wiig, *Exp. Eye Res.* **1990**, *50*, 261.
[33] J. V. Jester, J. Ho-Chang, *Exp. Eye Res.* **2003**, *77*, 581.
[34] Y. M. Michelacci, *Braz. J. Med. Biol. Res.* **2003**, *36*, 1037.
[35] D. C. Paik, S. L. Trokel, L. H. Suh, *Cornea* **2018**, *37*, e49.
[36] S. L. Wilson, A. J. El Haj, Y. Yang, *J. Funct. Biomater.* **2012**, *3*, 642.
[37] J. A. West-Mays, D. J. Dwivedi, *Int. J. Biochem. Cell Biol.* **2006**, *38*, 1625.
[38] N. Garcia-Porta, P. Fernandes, A. Queiros, J. Salgado-Borges, M. Parafita-Mato, J. M. González-Méijome, *ISRN Ophthalmol.* **2014**, *2014*, 724546.1.
[39] K. E. Hamilton, D. C. Pye, *Optom. Vis. Sci.* **2008**, *85*, 445.
[40] C. E. Ghezzi, B. Marelli, F. G. Omenetto, J. L. Funderburgh, D. L. Kaplan, *PLoS One* **2017**, *12*, e0169504.
[41] J. M. Dias, N. M. Ziebarth, *Exp. Eye Res.* **2013**, *115*, 41.
[42] Y. Zeng, J. Yang, K. Huang, Z. Lee, X. Lee, *J. Biomech.* **2001**, *34*, 533.
[43] W. M. Petroll, M. Miron-Mendoza, *Exp. Eye Res.* **2015**, *133*, 49.
[44] P. Bhattacharjee, B. L. Cavanagh, M. Ahearne, *Sci. Rep.* **2020**, *10*.
[45] Q. Guo, J. M. Phillip, S. Majumdar, P.-H. Wu, J. Chen, X. Calderón-Colón, O. Schein, B. J. Smith, M. M. Trexler, D. Wirtz, J. H. Elisseeff, *Biomaterials* **2013**, *34*, 9365.
[46] N. Lakshman, W. M. Petroll, *Invest. Ophthalmol. Visual Sci.* **2012**, *53*, 1077.
[47] J. Chen, L. J. Backman, W. Zhang, C. Ling, P. Danielson, *ACS Biomater. Sci. Eng.* **2020**, *6*, 5162.
[48] D. A. Vargas, I. G. Gonçalves, T. Heck, B. Smeets, L. Lafuente-Gracia, H. Ramon, H. Van Oosterwyck, *Front. Bioeng. Biotechnol.* **2020**, *8*, 459.
[49] H. Hong, S. M. Park, D. Kim, S. J. Park, D. S. Kim, *J. Biomed. Mater. Res., Part B* **2020**, *108*, 1000.
[50] M. Winkler, D. Chai, S. Kriling, C. J. Nien, D. J. Brown, B. Jester, T. Juhasz, J. V. Jester, *Invest. Ophthalmol. Visual Sci.* **2011**, *52*, 8818.
[51] A. I. Teixeira, P. F. Nealey, C. J. Murphy, *J. Biomed. Mater. Res., Part A* **2004**, *71*, 369.
[52] P. Bhattacharjee, B. L. Cavanagh, M. Ahearne, *Colloids Surf., B* **2020**, *190*, 110971.
[53] D. Karamichos, X. Q. Guo, A. E. K. Hutcheon, J. D. Zieske, *Invest. Ophthalmol. Visual Sci.* **2010**, *51*, 1382.
[54] M. Kitagawa, A. M. Okamura, B. T. Bethea, V. L. Gott, W. A. Baumgartner, *Lecture Notes in Computer Science, (Lecture Notes in Artificial Intelligence and Lecture Notes in Bioinformatics)*, Springer, Berlin **2002**, Vol. *2488*, pp. 155–162.
[55] H. Goodarzi, K. Jadidi, S. Pourmotabed, E. Sharifi, H. Aghamollaei, *Int. J. Biol. Macromol.* **2019**, *126*, 620.
[56] W. Liu, K. Merrett, M. Griffith, P. Fagerholm, S. Dravida, B. Heyne, J. C. Scaiano, M. A. Watsky, N. Shinozaki, N. Lagali, R. Munger, F. Li, *Biomaterials* **2008**, *29*, 1147.
[57] P. Fagerholm, N. S. Lagali, J. A. Ong, K. Merrett, W. B. Jackson, J. W. Polarek, E. J. Suuronen, Y. Liu, I. Brunette, M. Griffith, *Biomaterials* **2014**, *35*, 2420.
[58] M. Mirazul Islam, V. Cėpla, C. He, J. Edin, T. Rakickas, K. Kobuch, Ž. Ruželė, W. Bruce Jackson, M. Rafat, C. P. Lohmann, R. Valiokas, M. Griffith, *Acta Biomater.* **2015**, *12*, 70.
[59] R. A. B. Crabb, E. P. Chau, M. C. Evans, V. H. Barocas, A. Hubel, *Tissue Eng.* **2006**, *12*, 1565.
[60] B. Jue, D. M. Maurice, *J. Biomech.* **1986**, *19*, 847.
[61] K. Merrett, P. Fagerholm, C. R. Mclaughlin, S. Dravida, N. Lagali, N. Shinozaki, M. A. Watsky, R. Munger, Y. Kato, F. Li, C. J. Marmo, M. Griffith, *Invest. Ophthalmol. Visual Sci.* **2008**, *49*, 3887.
[62] M. Rafat, F. Li, P. Fagerholm, N. S. Lagali, M. A. Watsky, R. Munger, T. Matsuura, M. Griffith, *Biomaterials* **2008**, *29*, 3960.
[63] X. Lei, Y.-G. Jia, W. Song, D. Qi, J. Jin, J. Liu, L. Ren, *ACS Appl. Bio. Mater.* **2019**, *2*, 3861.
[64] X. Duan, H. Sheardown, *Biomaterials* **2006**, *27*, 4608.
[65] H. J. Lee, G. M. Fernandes-Cunha, K.-S. Na, S. M. Hull, D. Myung, *Adv. Healthcare Mater.* **2018**, *7*, 1800560.
[66] M. G. Haugh, M. J. Jaasma, F. J. O'brien, *J. Biomed. Mater. Res., Part A* **2009**, *89A*, 363.
[67] D. Cherfan, E. E. Verter, S. Melki, T. E. Gisel, F. J. Doyle, G. Scarcelli, S. H. Yun, R. W. Redmond, I. E. Kochevar, *Invest. Ophthalmol. Visual Sci.* **2013**, *54*, 3426.
[68] C. C. Drechsler, A. Kunze, A. Kureshi, G. Grobe, S. Reichl, G. Geerling, J. T. Daniels, S. Schrader, *J. Tissue Eng. Regener. Med.* **2017**, *11*, 896.
[69] Y. Liu, L. Ren, Y. Wang, *Mater. Sci. Eng. C* **2013**, *33*, 196.
[70] Z. Wu, B. Kong, R. Liu, W. Sun, S. Mi, *Nanomaterials* **2018**, *8*, 124.
[71] J. I. Kim, J. Y. Kim, C. H. Park, *Sci. Rep.* **2018**, *8*, 1.
[72] C. Jiang, X. Wang, R. Gunawidjaja, Y.-H. Lin, M. K. Gupta, D. L. Kaplan, R. R. Naik, V. V. Tsukruk, *Adv. Funct. Mater.* **2007**, *17*, 2229.
[73] M. C. Lee, D.-K. Kim, O. J. Lee, J.-H. Kim, H. W. Ju, J. M. Lee, B. M. Moon, H. J. Park, D. W. Kim, S. H. Kim, C. H. Park, *J. Biomed. Mater. Res., Part B* **2016**, *104*, 508.
[74] L. Guan, H. Ge, X. Tang, S. Su, P. Tian, N. Xiao, H. Zhang, L. Zhang, P. Liu, *Cells Tissues Organs* **2013**, *198*, 190.
[75] J. Chen, C. Yan, M. Zhu, Q. Yao, C. Shao, W. Lu, J. Wang, X. Mo, P. Gu, Y. Fu, X. Fan, *Int. J. Nanomed.* **2015**, *10*, 3337.
[76] P. Bhattacharjee, J. Fernández-Pérez, M. Ahearne, *Mater. Sci. Eng. C* **2019**, *105*, 110093.
[77] B. Aghaei-Ghareh-Bolagh, J. Guan, Y. Wang, A. D. Martin, R. Dawson, S. M. Mithieux, A. S. Weiss, *Biomaterials* **2019**, *188*, 50.
[78] K. Long, Y. Liu, W. Li, L. Wang, S. Liu, Y. Wang, Z. Wang, L. Ren, *J. Biomed. Mater. Res., Part A* **2015**, *103*, 1159.
[79] S. Krishnan, S. Sekar, M. F. Katheem, S. Krishnakumar, T. P. Sastry, *Artif. Organs* **2012**, *36*, 829.
[80] T. H. Van Essen, L. Van Zijl, T. Possemiers, A. A. Mulder, S. J. Zwart, C.-H. Chou, C. C. Lin, H. J. Lai, G. P. M. Luyten, M. J. Tassignon, N. Zakaria, A. El Ghalbzouri, M. J. Jager, *Biomaterials* **2016**, *81*, 36.
[81] H. Feng, X. Li, X. Deng, X. Li, J. Guo, K. Ma, B. Jiang, *RSC Adv.* **2019**, *10*, 875.
[82] K. Tonsomboon, D. G. T. Strange, M. L. Oyen, *Annu. Int. Conf. IEEE Eng. Med. Biol. Soc.* **2013**, *2013*, 6671.

[83] K. Tonsomboon, A. L. Butcher, M. L. Oyen, *Mater. Sci. Eng. C* **2017**, *72*, 220.
[84] L.-J. Luo, J.-Y. Lai, S.-F. Chou, Y.-J. Hsueh, D. H.-K. Ma, *Acta Biomater.* **2018**, *65*, 123.
[85] J.-Y. Lai, Li, Cho, Yu, *Int. J. Nanomed.* **2012**, *7*, 1101.
[86] J.-Y. Lai, *Int. J. Mol. Sci.* **2013**, *14*, 2036.
[87] J. B. Rose, L. E. Sidney, J. Patient, L. J. White, H. S. Dua, A. J. El Haj, A. Hopkinson, F. R. A. J. Rose, *J. Biomed. Mater. Res., Part A* **2019**, *107*, 828.
[88] C. Kilic Bektas, V. Hasirci, *Biomater. Sci.* **2020**, *8*, 438.
[89] G. K. Tummala, T. Joffre, V. R. Lopes, A. Liszka, O. Buznyk, N. Ferraz, C. Persson, M. Griffith, A. Mihranyan, *ACS Biomater. Sci. Eng.* **2016**, *2*, 2072.
[90] A. Khoushabi, A. Schmocker, D. P. Pioletti, C. Moser, C. Schizas, J. A. Månson, P. E. Bourban, *Compos. Sci. Technol.* **2015**, *119*, 93.
[91] A. Vega-Estrada, J. Silvestre-Albero, A. E. Rodriguez, F. Rodriguez-Reinoso, J. A. Gomez-Tejedor, C. M. Antolinos-Turpin, L. Bataille, J. L. Alio, *J. Ophthalmol.* **2016**, *2016*, 1.
[92] K. Tonsomboon, M. L. Oyen, *J. Mech. Behav. Biomed. Mater.* **2013**, *21*, 185.
[93] R. M. Gouveia, E. González-Andrades, J. C. Cardona, C. González-Gallardo, A. M. Ionescu, I. Garzon, M. Alaminos, M. González-Andrades, C. J. Connon, *Biomaterials* **2017**, *121*, 205.
[94] X. Wang, S. Majumdar, U. Soiberman, J. N. Webb, L. Chung, G. Scarcelli, J. H. Elisseeff, *Biomaterials* **2020**, *241*, 119880.
[95] M. Ahearne, J. Fernández-Pérez, S. Masterton, P. W. Madden, P. Bhattacharjee, *Adv. Funct. Mater.* **2020**, *30*, 1908996.
[96] A. Sorushanova, L. M. Delgado, Z. Wu, N. Shologu, A. Kshirsagar, R. Raghunath, A. M. Mullen, Y. Bayon, A. Pandit, M. Raghunath, D. I. Zeugolis, *Adv. Mater.* **2019**, *31*, 1801651.
[97] H. Hong, H. K. Kim, S. Han, H. Kim, D. Cho, D. S. Kim, *2018 IEEE Int. Conf. Cyborg and Bionic Systems, CBS 2018*, IEEE, Piscataway, NJ, USA **2018**, pp. 195–198.
[98] H. Hong, H. Kim, S. J. Han, J. Jang, H. K. Kim, D.-W. Cho, D. S. Kim, *Mater. Sci. Eng., C* **2019**, *103*, 109837.
[99] V. Kishore, R. Iyer, A. Frandsen, T.-U. Nguyen, *Biomed. Mater.* **2016**, *11*, 055008.
[100] J. Shi, H. Lian, Y. Huang, D. Zhao, H. Wang, C. Wang, J. Li, L. Ke, *Regen. Biomater.* **2020**, *7*, 619.
[101] F. S. Tenório, T. L. Amaral Montanheiro, A. M. I. Dos Santos, M. Silva, A. P. Lemes, D. B. Tada, *J. Appl. Polym. Sci.* **2021**, *138*, 49819.
[102] H. G. Sundararaghavan, G. A. Monteiro, N. A. Lapin, Y. J. Chabal, J. R. Miksan, D. I. Shreiber, *J. Biomed. Mater. Res., Part A* **2008**, *87*, 308.
[103] J. Rose, S. Pacelli, A. Haj, H. Dua, A. Hopkinson, L. White, F. Rose, *Materials* **2014**, *7*, 3106.
[104] C. Kilic Bektas, V. Hasirci, *J. Tissue Eng. Regener. Med.* **2018**, *12*, e1899.
[105] H. Hong, M.-I. Huh, S. M. Park, K.-P. Lee, H. K. Kim, D. S. Kim, *Biofabrication* **2018**, *10*, 045001.
[106] M. Ahearne, A. Coyle, *J. Mech. Behav. Biomed. Mater.* **2016**, *54*, 259.
[107] J. Wu, J. Rnjak-Kovacina, Y. Du, M. L. Funderburgh, D. L. Kaplan, J. L. Funderburgh, *Biomaterials* **2014**, *35*, 3744.
[108] D. I. Zeugolis, S. T. Khew, E. S. Y. Yew, A. K. Ekaputra, Y. W. Tong, L.-Y. L. Yung, D. W. Hutmacher, C. Sheppard, M. Raghunath, *Biomaterials* **2008**, *29*, 2293.
[109] L. A. Hapach, J. A. VanderBurgh, J. P. Miller, C. A. Reinhart-King, *Phys. Biol* **2015**, *12*, 061002.
[110] A. Agrawal, N. Rahbar, P. D. Calvert, *Acta Biomater.* **2013**, *9*, 5313.
[111] A. M. Jordan, S.-E. Kim, K. Van De Voorde, J. K. Pokorski, L. T. J. Korley, *ACS Biomater. Sci. Eng.* **2017**, *3*, 1869.
[112] R. E. Thompson, L. C. Boraas, M. Sowder, M. K. Bechtel, E. J. Orwin, *Tissue Eng., Part A* **2013**, *19*, 1564.
[113] J. R. Hassell, D. E. Birk, *Exp. Eye Res.* **2010**, *91*, 326.
[114] X. Sun, X. Yang, W. Song, L. Ren, *ACS Omega* **2020**, *5*, 674.
[115] J. B. Lian, S. Morris, B. Faris, J. Albright, C. Franzblau, *BBA – Protein Struct.* **1973**, *328*, 193.
[116] L. M. Delgado, Y. Bayon, A. Pandit, D. I. Zeugolis, *Tissue Eng., Part B* **2015**, *21*, 298.
[117] G. S. Krishnakumar, S. Sampath, S. Muthusamy, M. A. John, *Mater. Sci. Eng. C* **2019**, *96*, 941.
[118] L. Gu, T. Shan, Y.-X. Ma, F. R. Tay, L. Niu, *Trends Biotechnol.* **2019**, *37*, 464.
[119] D. R. Eyre, M. A. Paz, P. M. Gallop, *Annu. Rev. Biochem.* **1984**, *53*, 717.
[120] J. M. Orban, L. B. Wilson, J. A. Kofroth, M. S. El-Kurdi, T. M. Maul, D. A. Vorp, *J. Biomed. Mater. Res., Part A* **2004**, *68*, 756.
[121] D. I. Zeugolis, P. P. Panengad, E. S. Y. Yew, C. Sheppard, T. T. Phan, M. Raghunath, *J. Biomed. Mater. Res., Part A* **2009**, *92*, 1310.
[122] Y. Wu, W. Song, Y. Tang, A. Elsheikh, Y. Shao, X. Yan, *Transl. Vision Sci. Technol.* **2019**, *8*, 27.
[123] Y. Wu, W. Song, Y. Tang, X. Yan, *Ophthalmic Res.* **2020**, *63*, 501.
[124] Y.-J. Hwang, J. Larsen, T. B. Krasieva, J. G. Lyubovitsky, *ACS Appl. Mater. Interfaces* **2011**, *3*, 2579.
[125] M. Y. Avila, V. A. Gerena, J. L. Navia, *Mol. Vision* **2012**, *18*, 1068.
[126] M. Y. Avila, M. Narvaez, J. P. Castañeda, *J. Cataract Refractive Surg.* **2016**, *42*, 1073.
[127] F. Everaerts, M. Torrianni, M. Hendriks, J. Feijen, *J. Biomed. Mater. Res., Part A* **2007**, *85A*, 547.
[128] W. Liu, C. Deng, C. R. Mclaughlin, P. Fagerholm, N. S. Lagali, B. Heyne, J. C. Scaiano, M. A. Watsky, Y. Kato, R. Munger, N. Shinozaki, F. Li, M. Griffith, *Biomaterials* **2009**, *30*, 1551.
[129] M. Koulikovska, M. Rafat, G. Petrovski, Z. Veréb, S. Akhtar, P. Fagerholm, N. Lagali, *Tissue Eng., Part A* **2015**, *21*, 1116.
[130] D. V. Bax, N. Davidenko, D. Gullberg, S. W. Hamaia, R. W. Farndale, S. M. Best, R. E. Cameron, *Acta Biomater.* **2017**, *49*, 218.
[131] R. A. B. Crabb, A. Hubel, *Tissue Eng., Part A* **2008**, *14*, 173.
[132] F. Raiskup, E. Spoerl, *Ocul. Surf.* **2013**, *11*, 65.
[133] N. Bekesi, I. E. Kochevar, S. Marcos, *Invest. Ophthalmol. Visual Sci.* **2016**, *57*, 992.
[134] U. Cheema, R. A. Brown, *Adv. Wound Care* **2013**, *2*, 176.
[135] Z. Cui, Q. Zeng, S. Liu, Y. Zhang, D. Zhu, Y. Guo, M. Xie, S. Mathew, D. Cai, J. Zhang, J. Chen, *Acta Biomater.* **2018**, *75*, 183.
[136] S. Schrader, J. Witt, G. Geerling, *Acta Ophthalmol.* **2018**, *96*, e757.
[137] X. Xiao, S. Pan, X. Liu, X. Zhu, C. J. Connon, J. Wu, S. Mi, *J. Biomed. Mater. Res., Part A* **2014**, *102*, 1782.
[138] B. Kong, W. Sun, G. Chen, S. Tang, M. Li, Z. Shao, S. Mi, et al, *Sci. Rep.* **2017**, *7*, 1.
[139] D. Phu, L. S. Wray, R. V. Warren, R. C. Haskell, E. J. Orwin, *Tissue Eng., Part A* **2011**, *17*, 799.
[140] L. S. Wray, E. J. Orwin, *Tissue Eng., Part A* **2009**, *15*, 1463.
[141] M. J. Fullana, G. E. Wnek, *Drug Delivery Transl. Res.* **2012**, *2*, 313.
[142] B. Dong, O. Arnoult, M. E. Smith, G. E. Wnek, *Macromol. Rapid Commun.* **2009**, *30*, 539.
[143] Q. Jiang, N. Reddy, S. Zhang, N. Roscioli, Y. Yang, *J. Biomed. Mater. Res., Part A* **2013**, *101A*, 1237.
[144] R. Grant, J. Hallett, S. Forbes, D. Hay, A. Callanan, *Sci. Rep.* **2019**, *9*, 1.
[145] K. H. Sizeland, K. A. Hofman, I. C. Hallett, D. E. Martin, J. Potgieter, N. M. Kirby, A. Hawley, S. T. Mudie, T. M. Ryan, R. G. Haverkamp, M. H. Cumming, *Materialia* **2018**, *3*, 90.
[146] R. N. Palchesko, S. D. Carrasquilla, A. W. Feinberg, *Adv. Healthcare Mater.* **2018**, *7*, 1701434.
[147] J. Satapathy, S. Samant, P. Pattnaik, *Int. J. Psychosoc. Rehabil.* **2019**, *23*, 653.
[148] J. Wu, J. Rnjak-Kovacina, Y. Du, M. L. Funderburgh, D. L. Kaplan, J. L. Funderburgh, *Biomaterials* **2014**, *35*, 3744.
[149] S. Das, A. Ghosh, *J. Appl. Polym. Sci.* **2006**, *99*, 3077.

[150] T. Menovsky, J. F. Beek, M. J. C. Van Gemert, *Lasers Surg. Med.* **1997**, *20*, 64.
[151] M. Okuda, N. Ogawa, M. Takeguchi, A. Hashimoto, M. Tagaya, S. Chen, N. Hanagata, T. Ikoma, *Microsc. Microanal.* **2011**, *17*, 788.
[152] C. Lin, R. Ritch, S. Lin, M.-H. Ni, Y.-C. Chang, Y. Lu, H. Lai, F.-H. Lin, *Eur. Cells Mater.* **2010**, *19*, 50.
[153] T. H. Van Essen, C. C. Lin, A. K. Hussain, S. Maas, H. J. Lai, H. Linnartz, T. J. T. P. Van Den Berg, D. C. F. Salvatori, G. P. M. Luyten, M. J. Jager, *Invest. Ophthalmol. Visual Sci.* **2013**, *54*, 3224.
[154] M. Szekalska, A. Puciłowska, E. Szymańska, P. Ciosek, K. Winnicka, *Int. J. Polym. Sci.* **2016**, *2016*, 1.
[155] A. Isaacson, S. Swioklo, C. J. Connon, *Exp. Eye Res.* **2018**, *173*, 188.
[156] S.-H. Jun, S.-H. Lee, S. Kim, S.-G. Park, C.-K. Lee, N.- K. Kang, *Cellulose* **2017**, *24*, 5267.
[157] Z. Keskin, A. Sendemir Urkmez, E. E. Hames, *Mater. Sci. Eng. C* **2017**, *75*, 1144.
[158] R. Hobzova, M. Duskova-Smrckova, J. Michalek, E. Karpushkin, P. Gatenholm, *Polym. Int.* **2012**, *61*, 1193.
[159] G. F. Picheth, C. L. Pirich, M. R. Sierakowski, M. A. Woehl, C. N. Sakakibara, C. F. De Souza, A. A. Martin, R. Da Silva, R. A. De Freitas, *Int. J. Biol. Macromol.* **2017**, *104*, 97.
[160] R. V. Sepúlveda, F. L. Valente, E. C. C. Reis, F. R. Araújo, R. B. Eleotério, P. V. S. Queiroz, A. P. B. Borges, *Pesq. Vet. Bras.* **2016**, *36*, 986.
[161] C. Zhang, J. Cao, S. Zhao, H. Luo, Z. Yang, M. Gama, Q. Zhang, D. Su, Y. Wan, *Cellulose* **2020**, *27*, 2775.
[162] X. W. Tan, B. Thompson, A. Konstantopoulos, T. W. Goh, M. Setiawan, G. H.-.F. Yam, D. Tan, K. A. Khor, J. S. Mehta, *Invest. Ophthalmol.Visual Sci.* **2015**, *56*, 6605.
[163] X. Wang, S. Majumdar, U. Soiberman, J. N. Webb, L. Chung, G. Scarcelli, J. H. Elisseeff, *Biomaterials* **2020**, *241*, 119880.
[164] M. Castilho, G. Hochleitner, W. Wilson, B. Van Rietbergen, P. D. Dalton, J. Groll, J. Malda, K. Ito, *Sci. Rep.* **2018**, *8*, 1.
[165] A. M. Jordan, S.-E. Kim, K. Van De Voorde, J. K. Pokorski, L. T. J. Korley, *ACS Biomater. Sci. Eng.* **2017**, *3*, 1869.
[166] T. Horeman, E.-J. Meijer, J. J. Harlaar, J. F. Lange, J. J. Van Den Dobbelsteen, J. Dankelman, *PLoS One* **2013**, *8*, e84466.
[167] L. L. Roybal, C. M. Blattner, J. Young, W. Lear, *JAAD Case Rep.* **2020**, *6*, 109.
[168] A. Handelman, Y. Keshet, E. Livny, R. Barkan, Y. Nahum, R. Tepper, *Int. J. Comput. Assisted Radiol. Surg.* **2020**, *15*, 1359.
[169] A. Dubrowski, R. Sidhu, J. Park, H. Carnahan, *Am. J. Surg.* **2005**, *190*, 131.
[170] C. Lee, Y. H. Park, C. Yoon, S. Noh, C. Lee, Y. Kim, H. C. Kim, H. H. Kim, S. Kim, *Med. Biol. Eng. Comput.* **2015**, *53*, 253.
[171] S. Pandey, V. Sharma, *Indian J. Ophthalmol.* **2019**, *67*, 988.
[172] Z. Hancox, S. Heidari Keshel, S. Yousaf, M. Saeinasab, M.-A. Shahbazi, F. Sefat, *Biomater. Sci.* **2020**, *8*, 6469.

Nello Formisano is a postdoctoral researcher at MERLN Institute for Technology-Inspired Regenerative Medicine at Maastricht University where he works on the bioengineering of materials, tissues and cell culture platforms that can be used for the treatment of corneal disease. He obtained his Ph.D. from the University of Bath studying electrochemical biosensors and his interests include 3D cell environment and bioengineering techniques for in vitro models.

Cas van der Putten is a Ph.D. candidate at the Department of Biomedical Engineering at Eindhoven University of Technology. His main research interests focus on cell-matrix interactions and how this interplay can be used in the fields of tissue engineering and regenerative medicine.

Rhiannon Grant is a postdoctoral researcher in the MERLN Institute for Technology-Inspired Regenerative Medicine at Maastricht University. She received her Ph.D. in bioengineering from The University of Edinburgh in 2019. Her research interests focus on the development of in vivo mimicking microenvironments, biomaterials for cell culture and enabling the adoption of these technologies in a clinical setting.

Stefan Giselbrecht is an assistant professor at the MERLN Institute for Technology-Inspired Regenerative Medicine at Maastricht University (The Netherlands). He holds a diploma in biology from the University of Saarbrücken (Germany) and received his Ph.D. in engineering science from the Technical University of Karlsruhe (now Karlsruhe Institute of Technology, Germany). His current research interests are focused on the development of microengineered and microfluidic platforms for advanced 3D in vitro models.